Universidade do Porto

FEUP Faculdade de Engenharia

Computational Methods for fMRI image Processing and Analysis

Gabriela Queirós

July 2013

Computational Methods for fMRI image Processing and Analysis

Measuring of the distance between a functional activation zone and the edge of a brain tumour

Dissertation presented to obtain the Master's degree in Biomedical Engineering

Gabriela Coelho de Pinho Queirós

Supervisor:

Doutor João Manuel R. S. Tavares

Associate Professor of the Department of Mechanical Engineering, Faculdade de Engenharia da Universidade do Porto

Co-Supervisor:

Doutor Mário António Basto Forjaz Secca

Associate Professor at Faculdade de Ciências e Tecnologia da Universidade Nova de Lisboa

“Success is not final, failure is not fatal:

it is the courage to continue that counts.”

Winston Churchill

Acknowledgments

I would like to acknowledge Professor Doutor João Manuel R. S. Tavares, for the support and availability during this work.
I would also like to acknowledge Professor Doutor Mário Secca, for the support during this work.
And to my family and friends, for all the patience, strength and unconditional support over these last years.

Abstract

The human brain is the principal organ of the central nervous system and the control centre of many voluntary and involuntary activities of the body and as such is the main responsible for higher and complex functions such as sensory perception, memory, consciousness, attention, thinking, language, movement and also emotions. So in order to prevent damage to this organ and its functions, when brain tumours occur that could influence its performance, the diagnosis and treatment is fundamental and indispensable.

Functional Magnetic Resonance Imaging is an application of the Magnetic Resonance Imaging referred to the use of this technology to detect localized changes in blood flow and blood oxygenation in the brain that occur in response to neural activity and has been developed with the goal of mapping the human brain and used to investigate the brain functions such as vision, language, motor and cognitive.

The main objective of this thesis was to develop a method, using two different software's, for measuring the distance between the centres of mass of brain activation areas and of the nearest edge of a brain tumour.

In order to perform the analysis of data gathered in the fMRI exams there were predefined steps to be used: image pre-processing (motion correction, temporal correction, spatial smoothing), image enhancement (spatial domain and frequency domain), image segmentation and statistical analysis of the functional data and this programming was done using the software's FSL and MATLAB to obtain the final results.

Resumo

O cérebro humano é o principal órgão do sistema nervoso central e o centro de controlo de muitas atividades voluntárias e involuntárias do organismo e, como tal, é o principal responsável por funções muito complexas como a perceção sensorial, memória, consciência, atenção, pensamento, linguagem, movimento e emoções. Então a fim de evitar danos neste órgão e nas suas funções, quando os tumores cerebrais ocorrem, que poderiam influenciar o seu desempenho, o diagnóstico e o tratamento são fundamentais e indispensáveis.

A Ressonância Magnética Funcional é uma aplicação da Ressonância Magnética que se refere à utilização desta tecnologia para detetar mudanças localizadas no fluxo sanguíneo e oxigenação do sangue no cérebro que ocorre em resposta a atividade neuronal e foi desenvolvida com a finalidade de mapear o cérebro humano e para investigar as funções cerebrais, tais como a visão, linguagem, motora e cognitiva.

O principal objetivo da presente tese foi desenvolver um método, utilizando dois softwares diferentes, para medir a distância entre os centros de massa das zonas de ativação do cérebro e a borda mais próxima de um tumor cerebral.

Para realizar a análise dos dados recolhidos nos exames de ressonância magnética existem etapas pré-definidas a serem utilizadas: pré-processamento de imagens (correção de movimento, correção temporal suavização espacial), realce de imagens (domínio espacial e no domínio da frequência), segmentação de imagens e análise estatísticas dos dados funcionais e esta programação foi feita utilizando os softwares FSL e MATLAB para a obtenção dos resultados finais.

Index

List of Figures

List of Tables

Glossary

A-D – Analog-Digital

AFNI – Analysis of Functional NeuroImages

B_0 – Magnetic field

BET – Brain Extraction Tool

BOLD – Blood Oxygenation Level Dependent

CT – Computed Tomography

dHb – Deoxyhemoglobin

Dicom – Digital Imaging and Comunication in Medicine

ET – Echo Time

FAST – FMRIB's Automated Segmentation Tool

FEAT – FMRI Expert Analysis Tool

FID – Free induction decay

FLAIR – Fluid attenuated inversion recovery

FLIRT – FMRIB's Linear Image Registration Tool

fMRI – Functional magnetic resonance imaging

FOV – Field of view

FSL – FMRIB Software Library

FWHM – Full Width at Half Maximum

HbO_2 – Oxyhemoglobin

M_0 – Magnetization moment

MarsBaR – Marseille Boite à Région d'Intéret

MCFLIRT – Motion correction FMRIB's Linear Image Registration Tool

M_L – Longitudinal magnetization

MRI – Magnetic resonance imaging

Mxy – Transversal magnetization

Nifti – Neuroinformatics Technology Initiative

NMR – Nuclear Magnetic Resonance

PET – Positron Emission Tomography

RF – Radiofrequency

RT – Repetition time

SNR – Signal to noise ratio

SPM – Statistical Parametric Mapping

SUSAN – Smallest Univalue Segment assimilating Nuclues

1. Introduction

1.1. Motivation and goals

1.2. Dissertation overview

1.3. Major Contributions

Biomedical engineering brings together principles of engineering, medicine, physics, chemistry and biology with the ultimate goal of improving health care available to society. Combining knowledge from the various disciplines, biomedical engineers are able to design instruments, devices and computational tools as well as medical studies and research to acquire and develop knowledge for the resolution of multiple issues.

The area of Medical Imaging makes possible the acquisition of information on the physiology and anatomy of internal organs in a non-invasive mean throughout various techniques such as Magnetic Resonance Imaging (MRI), X-Ray, Computed Tomography (CT) and Positron Emission Tomography (PET). Thanks to this it is possible the early detection of diseases, a better coordination of medical treatments and even a better general knowledge of the molecular activities of living organisms.

The Biomedical Engineering thus has a key role in this area through the design, construction and analysis of medical imaging systems, which allows it to be an area with huge expansion in the fields of instrumentation and computational analysis [1].

The history of Imaging had its beginning many centuries ago with the discovery of fundamental concepts of physics, biology and chemistry. But the real impetus was given in 1895 by the German physicist Wilhelm C. Roentgen, with the accidental discovery of X-Ray which allowed the obtainment of the first medical imaging, a radiograph of the left hand of his wife. For several decades the X-Ray was a source of medical imaging and by the 30s it was already used to view most of the human organs.

In 1942, Karl T. Dussik, Austrian neurologist reported the first use of ultrasound as a diagnostic tool and in 1968 the gynaecologist and obstetrician Stuart Campbell published an improved method of ultrasound images that would later be used as a current tool for the examination of fetuses during pregnancy [1].

Subsequently the X-Ray expanded to CT Streaming and allowed Godfrey Hounsfield to construct the first CT scanner, in 1972, by using the mathematical methodology of image reconstruction developed by Allan Cormack, during the previous decade. These findings owned these two scientists the Nobel Prize for Medicine in 1979.

The phenomenon of Nuclear Magnetic Resonance (NMR) was first described by Felix Bloch and Edward Purcell, in the 50s but it was only in 1971 that the first work of applying NMR to obtain medical images emerged [2]. This work developed by American researcher Raymond V. Damadian showed that the magnetic relaxation time of human tissues differed from the tumours.

In the early 80's MRI was considered as a new way to take pictures inside the human body and this spurred researchers to turn this technology in a sophisticated and robust method of obtaining these images through the use of scanners as the one in Figure 1.1.

Figure 1.1 – Siemens MAGNETOM Symphony 1.5T MRI System Scanner, USA. **[1]**

Developments in the magnetic technology such as the appearance of superconducting electromagnets made it possible to obtain images with better quality and also the appearance of "open" MRI with scanners as shown in Figure 1.2 that made possible the increasingly acceptance of this technology by patients.

Figure 1.2 – Siemens MAGNETOM C! 0.35T ”Open” MRI Scanner, USA. **[1]**

In 1990, Seiji Ogawa, Japanese biophysical, discovered in works with the partnership of AT & T's Bell Laboratories, that deoxyhemoglobin (dHb) when under the influence of a magnetic field, increased the strength of the field in its vicinity while the oxyhemoglobin (HbO_2) did not. It was the discovery of this phenomenon that led to the development of Functional Magnetic Resonance Imaging (fMRI), which allowed the acquisition of images of functioning and the study of their various functions.

The improvement of these technologies has also been possible with the development of computational analysis area, by creating increasingly sophisticated algorithms that enable the extraction of structural and functional information for volumetric measurement, processing, display and analysis of images [1].

1.1. Motivations and Goals

The Medical Imagiology field has, along the years, been gaining a big relevance. Its development has evolved at such fast pace that the knowledge in the anatomy and physiology of the human body became increasingly fast, detailed and less expensive. Alongside this development, the technological developments, mainly the computational ones, allowed the evolution of tools and algorithms increasingly faster and more objective.

The fMRI studies and developments allowed the acquisition of knowledge inherent to the technic and also to the image processing tools needed during the development of this thesis.

Considering these aspects the goals of this thesis were:

- Learning how to acquire functional MRI scans;
- Learn to analyse the functional MRI images of the brain;
- Acknowledge the theory of image processing (correction of motion, co-registration, segmentation, etc.);
- Knowing how to work with FMRIB Software Library (created by de Analysis Group, FMRIB, Oxford, UK) (FSL), and the Statistical Parametric Mapping (SPM) tool of MATLAB (created by members and collaborators of the *Wellcome Trust Centre of Neuroimaging*);

- Calculate the centre of mass of the activating zone - Varying the threshold values and measure the centre of mass for each case, reaching an average value for the activation;
- Study the automatic segmentation of the target lesion and study the possibility of having to make a manual segmentation in some cases;
- Determine in a three-dimensional volume the shortest distance between the mass centre of the activation zone and the edge of the lesion;

1.2. Dissertation overview

The following chapters present the theoretical and practical research done during the development of this thesis. It is structured in six more chapters that are briefly explained here:

- **Chapter 2 – The Brain:** in this chapter a description of the brain is provided. Hence, the chapter starts with the explanation of the brain anatomy, followed by the physiologic events that happen in this organ. Then, the chapter presents a description of the brain activation areas and their functions and subsequently the cancer pathologies more frequent in this organ and the diagnose criteria chosen by doctors.
- **Chapter 3 – Magnetic Resonance Imaging:** this chapter is a presentation of the MRI technique explaining the physical principles and instrumentation required for its use. Thereafter is explained the process of mapping the MRI signal as well as the formation, production methods and properties of the images from this technique, and finally its main purpose applications.
- **Chapter 4 – Functional MRI:** this chapter aims to explain the technique of functional magnetic resonance imaging and its principles, scanning methodologies, explain how to process an experimental study of fMRI and how this technique is used for the study of brain tumours.

- **Chapter 5 – Image Processing and Analysis:** here is explained the complete procedure of analysis and processing of images used in this work. It was intended to clarify the methods of pre-processing, enhancement, segmentation and feature extraction to be used and their subsequent application to fMR images.
- **Chapter 6 – Implementation, results and discussion:** at this stage is presented the software's used throughout this thesis, their operating mode, the more practical aspects of their implementation and the data base of images used, and is explained all the implementation of the practical part of the thesis, as well as their results and their consequent discussion.
- **Chapter 7 – Conclusions and future perspectives:** finally we present the final conclusions, as well as the possible future prospects of implementing an automatic method for the analysis and measurement of brain tumours and their distance to the areas of brain activation.

1.3. Major contributions

The major contribution of this thesis was to develop a method, using two different software's, for measuring the distance between the centres of mass of brain activation areas and of the nearest edge of a brain tumour, and comparison of both approaches, diagnosed in fMRI clinical exams, in order to obtain a quantitative value to provide to the surgeon for surgical planning.

2. The Brain

2.1. Introduction

This chapter aims to give a brief explanation of the anatomy and physiology of the brain, the most complex and vital organ, centre of the human central nervous system, as well as their areas of activation and functions. Some fundamental knowledge about brain tumours will also be presented, necessary for the study in question.

2.2. Anatomy and Physiology of the brain

The human brain, shown in Figure 2.1, is the principal organ of the central nervous system and the control centre of many voluntary and involuntary activities of the body and as such is responsible for actions as complex as thinking, memory, emotion and language. In the adult this organ may have about 12 billion neurons (nerve cells).

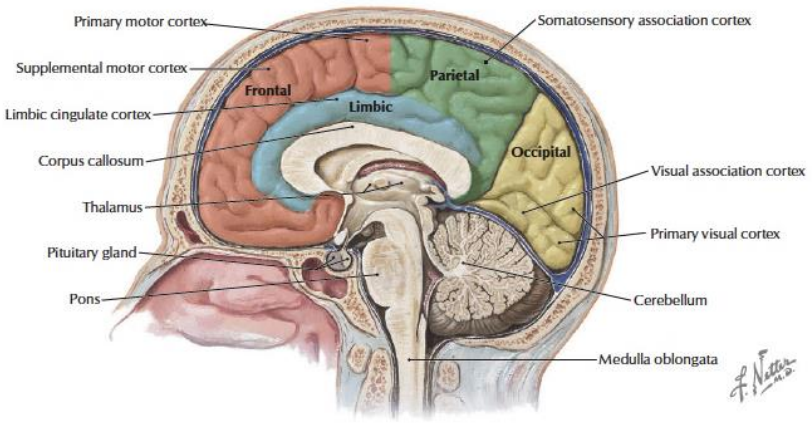

Figure 2.1 – Medial aspect of the brain and brainstem **[3]**

It is divided into two hemispheres, left and right, where the functional areas are differentiated, however there is no general agreement on the definition and marking of the boundaries between each of these areas and the absence of these anatomical definitions leads to the existence of several subdivisions of the cerebral cortex. The left hemisphere is responsible for logical thinking and communicative competences, with highly specialized areas

such as Broca's area (B), responsible for motor speech, and Wernicke's area (W) responsible for verbal comprehension, while the right hemisphere is responsible for symbolic thought and creativity. The corpus callosum, located deep in the sagittal fissure, is the structure that connects the two cerebral hemispheres and is responsible for the exchange of information between different areas of the cerebral cortex. The motor cortex is responsible for the control and coordination of voluntary movements. The motor cortex of the left hemisphere controls the right side of the body and the motor cortex of the right hemisphere controls the left side of the body. The premotor cortex, responsible for the motor learning and the precision movements, is located in front of the area of the motor cortex. The cerebellum is primarily responsible for the overall coordination of motor skills and balance. The axis formed by the adeno-hypophysis and hypothalamus, is responsible for the homeostatic functions of the organism (cardio-respiratory, circulatory, etc.).

The cerebral cortex is divided into four areas called cerebral lobes, with differentiated and specialized functions:

- The **frontal lobe**, located in the forehead, includes the motor cortex, the premotor and the prefrontal cortex and is responsible for planning actions and movements as well as functions that may include abstract and creative thinking, fluency of thought and language, emotional and affective responses, will and selective attention;
- The **occipital lobe**, in the neck region, is covered by the cerebral cortex, also referred to as the visual cortex, and consists of several sub-areas specialized on processing the colour vision, movement, depth and distance;
- The **parietal lobe**, at the top centre of the head comprises two subdivisions - the anterior designated by somatosensory cortex, with the sensations related functions (touch, pain, temperature, etc.). And posterior which is a secondary area which analyses, interprets and integrates the information received by the previous area;
- And **temporal lobes**, in the lateral regions of the head above the ears, that have as main function the processing of auditory stimuli.

There is another map also widely used, based on the subdivision of the cerebral hemispheres in about 50 cytoarchitectonic areas (Figure 2.2), by Korbinian Brodmann's, which are divided into five major functional areas [4]:

- Limbic;
- Paralimbic;
- Heteromodal association;
- Unimodal association;
- Primary sensory-motor.

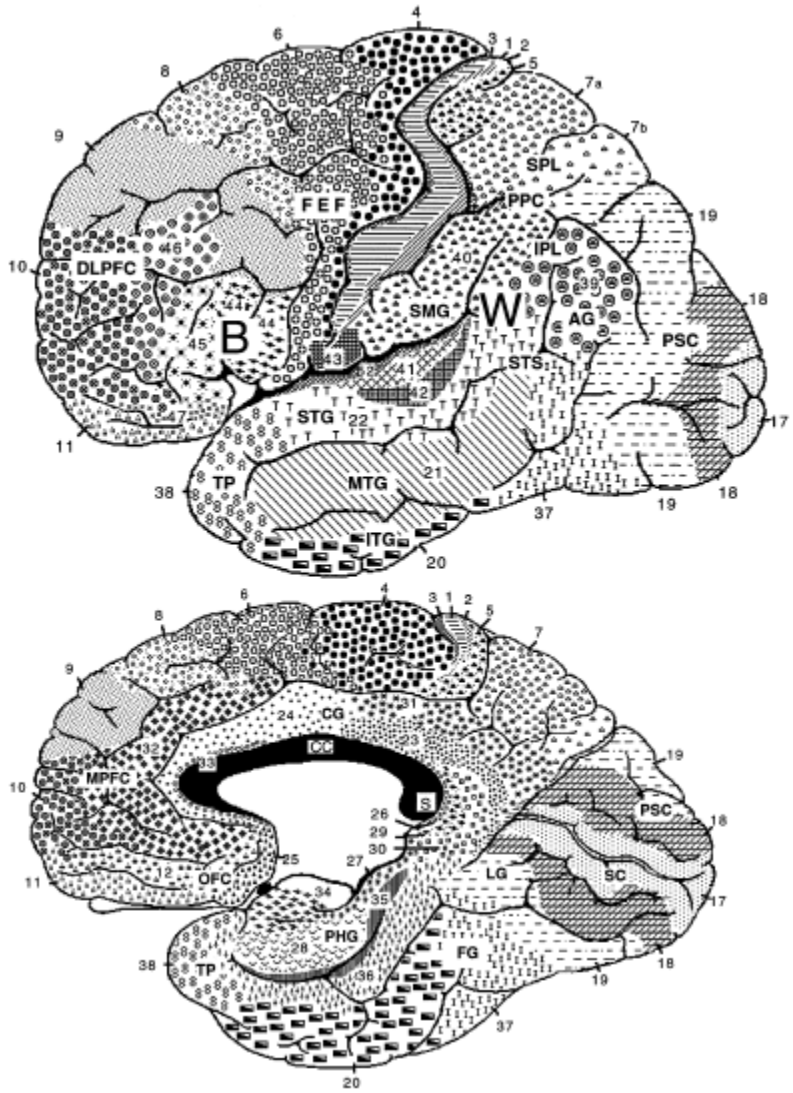

Figure 2.2 – Lateral (on top) and medial (on bottom) views of the cerebral hemispheres **[4]**

2.3. Brain Activation Areas

As it is known the cerebral cortex, with 2-4 mm of thickness, composed by an enormous number of neurons and their interconnections, is organized into lobes and is the main responsible for higher and complex functions such as sensory perception, memory, consciousness, attention, thinking, language, movement and also emotions.

For a better understanding, the cerebral cortex is classified by function into two different areas:

- The motor control areas – located in both hemispheres of the cortex they are responsible for the generation of movement. These areas are the primary motor cortex, which is located in the pre-central gyrus, and the premotor and motor areas (responsible for the staging of motor functions). Figure 2.3 shows the topographic organization of the motor cortex (the right half of the motor area controls the left side of the body, and vice versa). There is also the Broca area or the speech motor area (which communicates with the premotor and motor areas to determine the speech muscular movements).

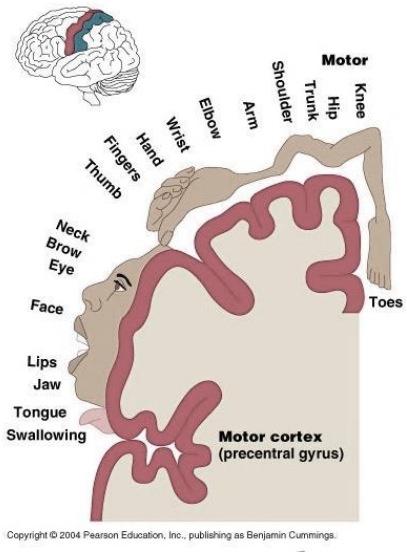

Figure 2.3 – Topographic organization of the primary motor cortex **[5]**

- The sensorial control areas – where the impulses responsible for senses are received and interpreted. The senses that are detected are responsible for smell, taste, hearing, vision and balance and somatic as touch, temperature, pressure, pain and proprioception. The areas responsible for this are the primary somatosensory cortex (topographically organized in Figure 2.4), the areas of taste, the olfactory cortex, primary auditory cortex, the primary visual cortex and association areas or secondary (somatosensory, auditory and visual). And there is also the Wernicke's sensory speech area (responsible for understanding and formulating speech) [4].

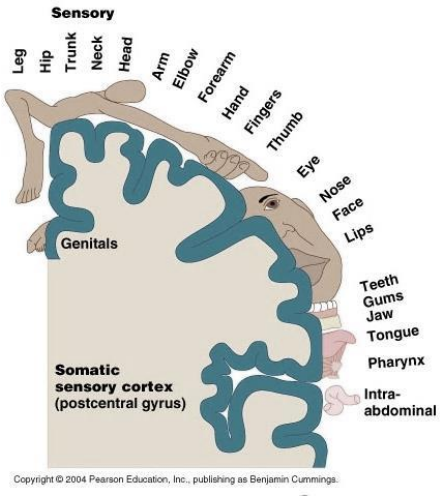

Figure 2.4 – Topographic organization of the primary somatosensory cortex **[5]**

Figure 2.5 shows a representation of these anatomical areas in the left cortex.

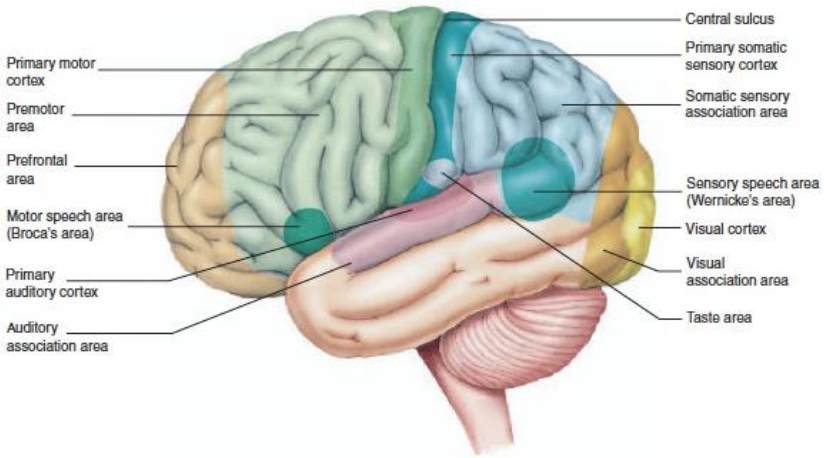

Figure 2.5 – Functional regions representation of the left side of the cerebral córtex **[6]**

- Other important functions, but whose areas are not as well defined, are the ones responsible for memory (temporal lobe) and for intelligence, judgment and behaviour (frontal lobe) as shown in Figure 8 [7].

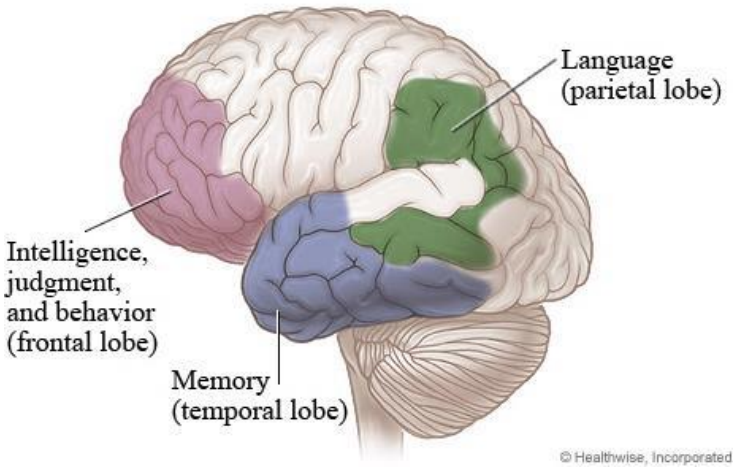

Figure 2.6 – Important functional areas of the brain **[8]**.

2.4. Brain Tumours

By definition, a brain tumour is an abnormal growth of cells in the brain tissues, inside the cranium, and according to Cancer Research UK, it is estimated that every year there are almost 445000 news cases of brain tumours worldwide [9].

These tumours are classified according to their origin. They are termed primary, if they begin to grow directly in the brain; otherwise they are secondary, if they spread to the brain from somewhere else in the body.

Primary brain tumours can be classified according to the type of tissue that origins it, they do not spread to other body sites, and can be malignant or benign. The most common ones are gliomas, which begin in the glial tissue and according to some histology statistics there are:

- Glioma 50,3%;
  - Glioblastoma 52%;
  - Astrocytoma 26%;
  - Oligodendroglioma, Ependymoma, etc 22%;
- Meningioma 20,9%;

- Pituitary 15%;
- Acoustic Neuroma, Nerve Sheath Tumors and Others 8% [9].

Secondary brain tumours, that are always malignant, are also known as metastatic cancer as they are the result of the spreading of other cancers that are growing somewhere else in the body and they are given the name of the origin cancer and these are the most common types of brain tumours (10 to 15% of cancer patients develop metastatic cancer to the brain). The derivations of these metastatic cancers percentage wise are:

- Lung 35%;
- Breast 20%;
- Melanoma 10%;
- Renal Cell 10%;
- Colon 5% [9].

These two types of tumours are potentially disabling and life threatening duo to the limited space inside the skull. Their growth increases intracranial pressure, and may cause edema, reduced blood flow, and displacement, with consequent degeneration, of healthy tissue that controls vital functions [10].

2.5. Treatment Options

Normally there is not one single procedure, it depends on the type, size and location of tumour, but for a good treatment plan there are some standard options like:

- Surgery;
- Radiation;
- Radiosurgery;
- Chemotherapy;
- Other option (ex: clinical trials).

When possible, the most recommended approach is the surgical removal, always maintaining the constraints of preservation of neurologic

functions and considering a previous evaluation of the patients health and surgical risks.

For high-grade gliomas the most common approach is radiation therapy.

Chemotherapy is a treatment option that is normally an addition to other treatments like surgery and radiation, especially for malignant gliomas.

For metastatic brain tumours there is a management approach that involves a combination of multiple treatments such as: corticosteroids, anticonvulsants, radiation therapy, radiosurgery and surgical resection [11].

2.6. Summary

The brain, as fundamental to human functioning organ is of extreme importance and the control centre of the human body, responsible for the control of the voluntary and involuntary activities that it preforms. It is divided in two hemispheres, each responsible for different functions. The more complex functions are controlled by the cerebral cortex, where the motor control and the sensorial control areas are located.

So in order to prevent damage to this organ and its functions, when lesions occur, such as tumours, that could influence its performance, the diagnosis and treatment is fundamental and indispensable.

3. Magnetic Resonance Imaging

3.1. Introduction

Magnetic Resonance Imaging (MRI) is an imaging technique capable of producing tomographic images of internal physical and chemical characteristics of a given body by external measurement of magnetic resonance signals. Tomography is a very important area of imaging, the Greek word tomos meaning "cut" but this enables obtaining images from inside the body without actually cutting it. Thus with the use of an MRI scanner is possible to obtain images and data sets representative of the multidimensional spatial distribution of a given physical quantity measure [12].

3.2. Technical principles

With the use of Magnetic Resonance Imaging technics it is possible to generate sectional 2-dimensional (2D) images with any orientation, volumetric 3D images and even 4D images of the spatio-spectral or spatio-temporal distributions. Another special feature of this technology is the nature of the signals used to form images since, unlike other technologies, it does not rely on particles with radiation to generate the signals received [12].

3.2.1. Instrumentation

The basic components of an MRI scanner are shown schematically in Figure 3.1:

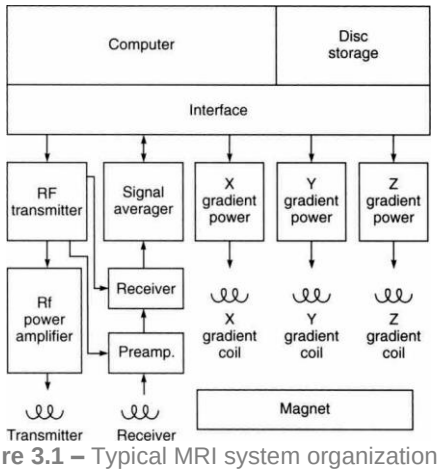

Figure 3.1 – Typical MRI system organization **[13]**

These instruments have static magnetic fields, uniform and strong (the strength can vary between 0.2T and 3T in clinical use) with three sets of coils, which have amplifiers and devices associated for correcting the current, necessary for spatial coding of the examining patient for producing a time varying magnetic gradient. The Radiofrequency (RF) transmitter transmits and receives the coils and amplifiers and the RF receivers are used for excitation of the nuclei and to receive the signals. The computer is used to control the scanner and to process and present the results (images, spectra, etc.). They also contain other devices and equipment for patient and safety systems monitoring [14].

- The **magnet** provides a stable and uniform magnetic field (B_0) (Figure 3.2);

The field B_0 of these scanners can be generated by resistive electromagnets, permanent magnets or superconducting magnets, being theses the most common and which due to the superconducting technology requires an own cooling system with liquid helium.

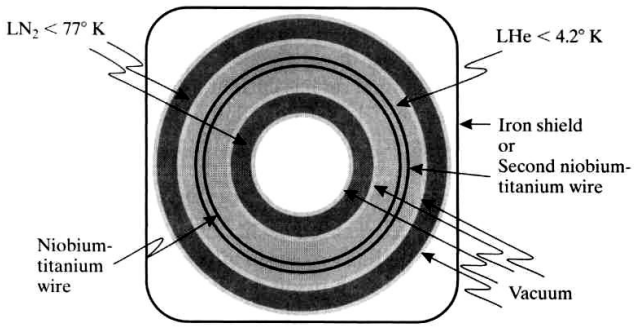

Figure 3.2 – Formation of a superconducting magnet scheme **[2]**

- The **RF transmitter** sends pulses of RF to the sample;

For the activation of nuclei this system that emits the signals consists of the RF transmitter itself, in a power amplifier and RF coils of transmission. A crystal that oscillates at a frequency of precession constitutes the transmitter itself.

- The **gradient system** generates time-varying magnetic fields;

It is this gradient system that is responsible for the ability of spatial coding the detected signals for the formation of images. This is due to the ability to locally control the magnetic field and to the use of three coils, which imposes linear variations in the magnetic field in any of the Cartesian directions.

- The **detection system** produces the output signal;

Its main function is to detect and generate the output signal to be processed by the computer and its structure is presented in accordance with the block diagram of Figure 3.3.

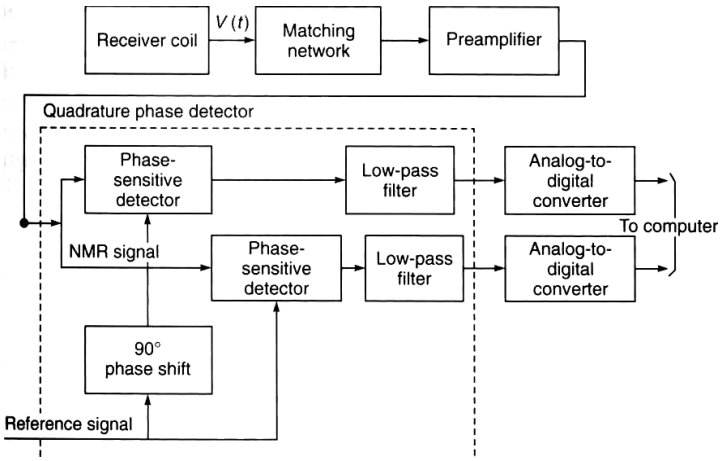

Figure 3.3 – Block diagram of detection system **[13]**

Here the receiving coil will act as an antenna to the floating nuclear magnetization of the sample and converts it into floating output voltage V(t). The coil is connected to a matching network that establishes the connection to the preamp to maximize the energy transferred to the amplifier and introduces a phase alternator for the signal. The preamp is a low noise amplifier that amplifies the signal and transfers it to a quadrature phase detector. This detection circuit receives the MR V(t) signal and the reference signal and multiplies it to obtain just an output. It also has a low pass filter for the removal of all components except the ones centred at zero. Lastly the signal is processed by an Analog-Digital (A-D) converter that transforms it in a series of data to be analysed in the computer.

- The **imager system** includes the computer for reconstruction and display of images (Figure 3.4) [13];

Figure 3.4 – Siemens Operation console of the MRI scanner **[2]**

In Figure 3.5 one can see how all these components are organized within an MRI scanner.

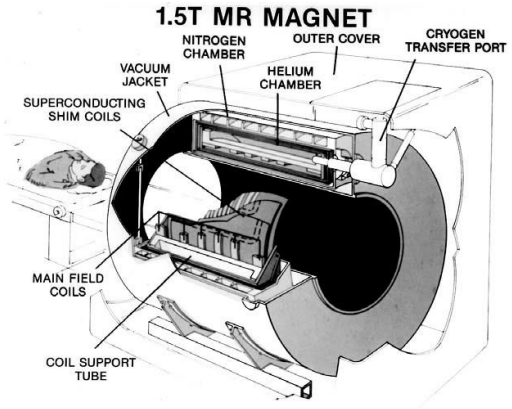

Figure 3.5 – Scheme of construction of an MRI scanner **[15]**

3.2.2. Physics

The protons and neutrons constituents of atomic nuclei possess a property called spin angular momentum (Φ) with magnitude and direction and which underlies the phenomenon of Nuclear Magnetic Resonance (NMR). This angular momentum or spin core may be considered as a result of rotational movement of the nucleus around its own axis which is illustrated in Figure 3.6. Hydrogen (1H) is the most abundant element in the body and hence the element of greatest interest for obtaining anatomical MR images enabling a stronger MRI signal.

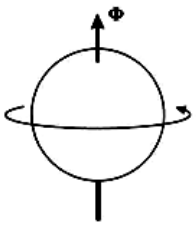

Figure 3.6 – Representation of the angular momentum of the nucleus **[2]**

Being the nucleus a charged particle, the spin is accompanied by a magnetic moment vector (μ) whose magnetization field representation is in Figure 3.7, and whose relationship with the spin angular momentum is given by the expression:

$$\boldsymbol{\mu} = \boldsymbol{\gamma \Phi} \qquad (3.1)$$

where γ is the gyromagnetic ratio which is a particular characteristic of the nuclei.

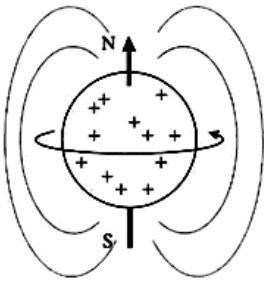

Figure 3.7 – Microscopic representation of the magnetization of a nucleus **[2]**

Table 1 shows the values of the gyromagnetic ratio of some common elements [2].

Table 3.1 – Values for the Gyromagnetic Ratio

	Gyromagnetic Ratio (MHz/T)
^{1}H	42.58
^{13}C	10.71
^{19}F	40.05
^{31}P	11.26

In the MRI the signal obtained is produced by the magnetic field of 1H, being this a signal too small to induce a current which can be detected by a coil.

Thus it becomes necessary the alignment of the protons so that it is possible to produce a magnetic moment large enough to be detected.

As the orientation of the protons is totally random as in Figure 3.8, its magnetic moment vectors will display multiple different directions which leads to the cancelling of each other. However, when they are placed under the influence of an external magnetic field (B_0) this aligns the spins in the same direction of the field but not all vectors have the same orientation. What happens is that the majority of the protons will align themselves in the same orientation of the field, which corresponds to a lower energy state (Parallel), and the others will line up in the opposite orientation, corresponding to a higher energy state (Anti-Parallel) as illustrated in Figure 3.9. This difference will cause a constant imbalance that will lead to a magnetization moment (M_0) of the tissue responsible for obtaining the MRI [12].

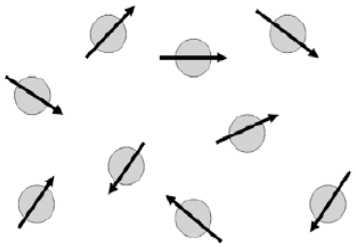

Figure 3.8 - Randomly representation of protons **[16]**

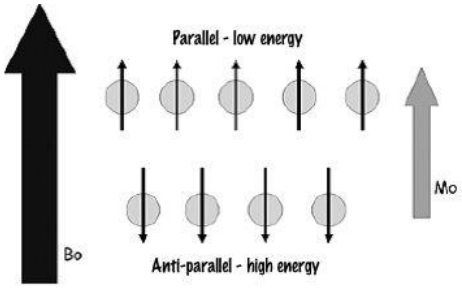

Figure 3.9 – Alignment of protons according to the M_0 direction after being placed in a strong magnetic field (B_0) **[16]**

The frequency at which the nuclei spin, as shown in Figure 3.10, also known as the Larmor frequency, or frequency of precession is proportional to

the gyromagnetic ratio and to the magnitude of the external magnetic field applied:

$$\boldsymbol{w = \gamma B_0} \tag{3.2}$$

Thus, by submitting the protons to action of a field of radio frequency as the frequency of precession we are going to cause a resonance phenomenon and this will mean that there is an increase in anti-parallel spins and that the spins are put into phase.

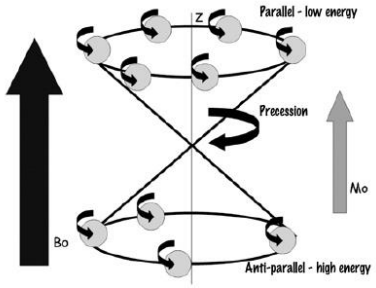

Figure 3.10 – Representing the precession frequency of protons around the axis z of strong magnetic field (B_0) **[16]**

The amplitude and the duration of the pulses of the frequency will determine the effects caused and the signal measured will be the transverse magnetization, signal that will only be possible to detect by coils that capture the radio frequency at the time that the protons exhibit the frequency of precession in phase, i.e., rotating around the longitudinal axis z [2].

At the moment that the RF is stopped, the transverse magnetization decreases and will disappear unlike the longitudinal magnetization that will increase, i.e., the protons will return to their equilibrium state emitting electromagnetic energy, phenomenon known as relaxation. This is a dynamic physical phenomenon in which the proton returns to its ground state.

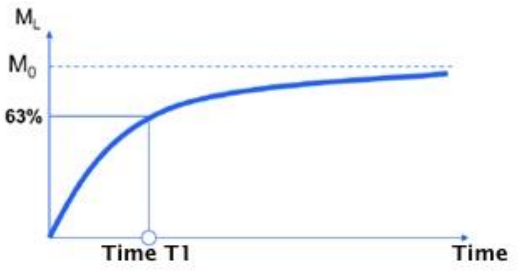

Figure 3.11 – Variation of longitudinal relaxation over time **[17]**

There are two types of relaxation, the longitudinal relaxation described by an exponential curve characterized by the time constant T1, during which protons are again aligned with the magnetic field. The curve illustrated in Figure 3.11 represents the variation of longitudinal relaxation over time, where one can see that T1 represents the time required for the longitudinal magnetization (M_L) to recover 63% of its initial value (M_0). The transverse relaxation is described by an exponential curve characterized by the time constant T2, which comes down to the exit of the protons of its phase state and the curve represented in Figure 3.12 shows the variation of magnetization in the transverse plane over time, where T2 represents the time required for the transverse magnetization (M_{XY}) to reach 32% of its initial value [17]. The transverse relaxation is more rapid than the longitudinal relaxation and these values are not related to magnetic field strength.

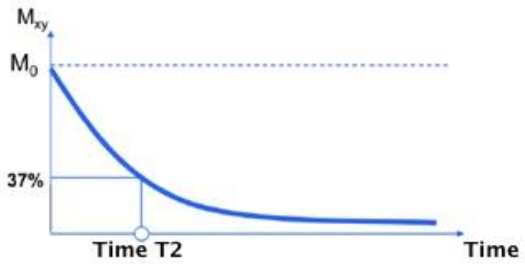

Figure 3.12 – Variation of magnetization in the transverse plane over time **[17]**

Table 2 shows some values of relaxation times, at the precession frequency of 20 MHz:

Table 3.2 – Approximate values of T1 and T2 for different tissues **[18]**

	T1 (ms)	T2 (ms)
Blood	1200	200
Muscle	500	35
Fat tissue	200	60
Water	3000	3000
White matter	790	90
Gray matter	920	100
Cerebrospinal liquid	4000	2000

After the RF pulse, many changes will occur in both magnetizations, the longitudinal magnetization increases, the transversal decreases and this process releases energy and to receive this signal an antenna is placed in the transverse plane (x0y) where an electric current is induced (Faraday's law). For a better understanding of the emission of this signal is necessary to specify the sequence of RF pulses called spin echo sequence. This is based on repetition of a pulse sequence of 90° and 180° consecutively and presents two parameters: TE / 2 and TE. The pattern of emission of these pulses is illustrated in Figure 3.13.

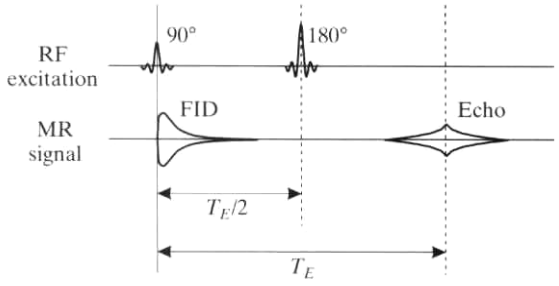

Figure 3.13 – Diagram of the pulse sequence for generating spin echoes **[2]**

The 90° pulse (TE / 2) causes the disappearance of the longitudinal magnetization and transverse growth and when it is turned off there is a decay of transverse magnetization, and the protons release the absorbed energy. This released energy will cause fluctuations in the frequency of the magnetic field, which induces an electric current, the signal. The frequency of this is constant but disappears over time, which translates into an exponential decay curve. The antennas receive the signal in the transverse plane due to variations of the transverse magnetization vector. When there is no magnetic gradient, occurs the free induction decay (FID), shown in Figure 3.14, which is caused by a decrease of transverse magnetization, loss of energy to the environment and reduction of the oscillation of the signal in the transverse plane. Because there is no magnetic gradient, the FID signal decreases more rapidly than T2 and is characterized by a time constant T2*. The time T2* is influenced by a particular type of spin-spin relaxation and the inhomogeneous static magnetic fields that accelerate the phase shift of the spins.

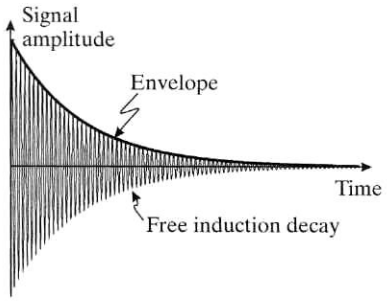

Figure 3.14 – Free induction decay caused by the transverse relaxation **[2]**

The impulse of 180º (TE) puts the spins in phase and inverts the inhomogeneous magnetic field and once applied with an RF with this pulse the spins go into phase and the transverse magnetization reappears and increases. After that, the spins move into a state of imbalance and the transverse magnetization decreases. When this state is fully achieved, the 180º pulse is sent and protons come back in phase. When switching off, the pulse of the 180º signal is emitted in the form of echoes. The difference in signal intensity depends on two factors, the Repetition Time (TR - which is the difference between the signal intensity between T1 tissues using two consecutive pulses, i.e. the difference between the longitudinal magnetization of different tissues) and the Echo Time (TE - which is the time between the 90º pulse and the echo). It could be chosen by the operator that indicates the type of the image (T1-weighted image, proton density and T2-weighted image – Figure 3.15) [18].

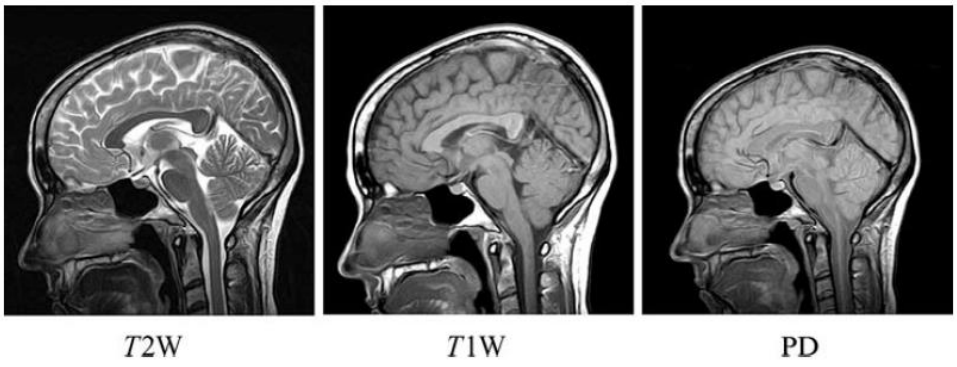

Figure 3.15 – MR images of sagittal brain cross section (T2W – T2 weighted, T1W – T1 weighted, PD – proton density) **[19]**

But there are other important factors that are needed to form an image.

For an object slice:

- The area that is acquired is the “field of view” – FOV, that is normally considered to be squared;
- The position is described by two-dimensions, the read-out (x) and the perpendicular phase-encode (y) direction.

Considering an object with a certain thickness (*d*), this is divided into volume elements (voxels) as shown in the Figure 3.16.

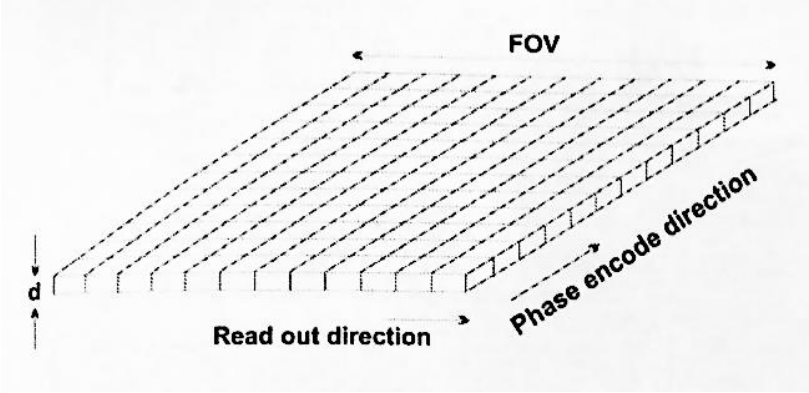

Figure 3.16 – Object slice divided into voxels **[20]**

in which the transverse directions is FOV/N and d in the longitudinal direction. The volume for each voxel is then given by:

$$\boldsymbol{V_{voxel}} = (\boldsymbol{FOV}/\boldsymbol{N})^2 \times \boldsymbol{d} \qquad (3.3)$$

The total magnetization vector of the voxel corresponds to the sum of all magnetizations inside a voxel and the length of this vector for each voxel is the brightness of a point in the image that is named pixel. The image is than obtained by gathering all the pixels together [20]. For a 3D image, the volume for each voxel is given by:

$$\boldsymbol{V_{voxel}} = \Delta \boldsymbol{x} \Delta \boldsymbol{y} \Delta \boldsymbol{z} \qquad (3.4)$$

Considering the patient as in the position showed in Figure 3.17, the magnetic field gradient will now be described along the z axis with:

$$\overrightarrow{\boldsymbol{B_z}} = \hat{\boldsymbol{z}}(\boldsymbol{B_0} + \boldsymbol{G_z z}) \qquad (3.5)$$

The amplitude of the MR signal is proportional to the number of spins in a plane perpendicular to the gradient and this is called frequency encoding. This

causes the resonance frequency to be proportional to the position of the spin and with association to the correspondent spatial location z, becoming:

$$\boldsymbol{\omega = \gamma B_z = \gamma B_0 + \gamma G_z z} \quad (3.6)$$

where B_0 is the magnetic field and G_z is the magnetic field gradient along the plane z.

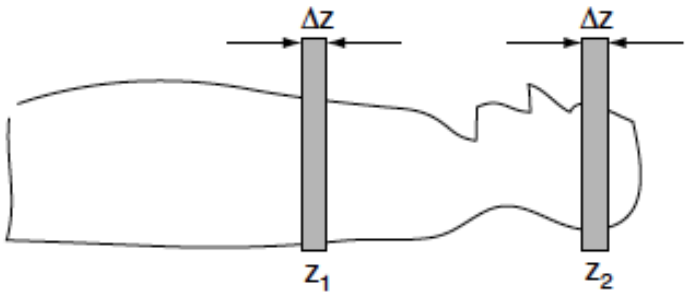

Figure 3.17 – side view of selected of axial image plane locations **[19]**

The one-dimensional magnetic field gradient along the z axis in B_0 indicates that the magnetic field is increasing in the z direction. Here the lengths of the vectors represent the magnitude of the magnetic field. The symbols for a magnetic field gradient in the x, y, and z directions are G_x, G_y, and G_z [19].

The large variety of available pulse sequences for imaging also reflects the variety of goals of imaging in different applications, such as the identification of pathological anatomy, and this requires a combination of sufficient spatial resolution to resolve small structures and sufficient signal contrast between pathological and healthy tissue to make the identification.

To obtain an image with many pulse sequences, the MR signal is operated by manipulation of both the RF and the gradient pulses in many ways. The RF pulses can be used as excitation pulses, to turn the magnetization from the longitudinal axis to the transverse plane, generating a detectable signal and as a refocusing pulse, to generate echoes of previous signals. The gradient pulses are used to eliminate unwanted signal and to encode information about the signals spatial distribution. Figure 3.18 shows a diagram with the pulse sequences in an acquisition event.

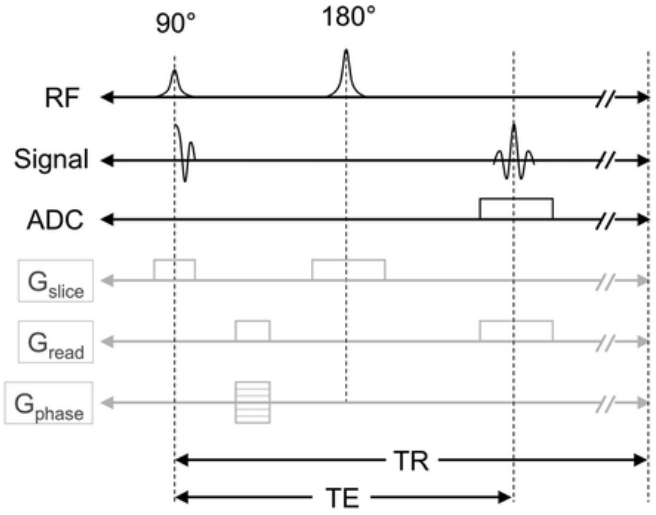

Figure 3.18 – Pulse sequence diagram **[21]**

Another of the main concepts behind this phenomenon is the spatial Fourier transform of the image, the k-space, which can be measured directly in the MR image. This concept allows the determination of parameters and features like the field of view (FOV), the spatial resolution and the speed of acquisition.

The k-space selection determines the basic parameters of the image, such as the FOV, spatial resolution, and speed of acquisition and the magnitude of the local MR signal, determines whether an image will show useful contrast between one tissue and another.

The Fourier transform theorem states that any function of position *x*, such as a profile through an image *I(x),* can also be expressed as a function of spatial frequencies *S(k)*, that is a sum of sine and cosine waves of different wavelengths and amplitudes that spread across all of *x*, where *k* is the inverse of the wavelength and so small k-values correspond to low spatial frequencies and long wavelengths. These two functions are related so that given one representation; the other can be obtained by calculation of the Fourier transform. Their mathematical relation can be seen in: [22].

$$\boldsymbol{S(k) = \int_{-\infty}^{\infty} I(x)\, e^{i2\pi kx} dx}$$

$$\boldsymbol{I(x) = \int_{-\infty}^{\infty} S(k)\, e^{-i2\pi kx} dk} \qquad (3.7)$$

This k-space representation is given such an importance because indeed is the *S(k)* that is actually measured and the *I(x)* is than reconstructed.

Now the image can be calculated by applying a 2D Fourier transform to the data acquires, by having the distribution in space being represented in terms of amplitudes of different spatial frequencies (*k*). So the MR image directly maps the k-space because the 2D Fourier transform will relate the image to the k-space representation.

In conclusion, the signals described above must be Fourier transformed to obtain the image representative of the location of spins. So during the MRI signal acquisition the phase and frequency encodings will vary and the correspondent signal will be recorded and used to fill the k-space. The phase encoding gradient will position the spin system at a specific line in the k-space array and the frequency encoding gradient will allow the movement of the spin system across that k-space line as function of the time.

Once the k-space is filled, the Fourier transformed data will be displayed as an image by conversion of the peaks to intensities of pixels representing the tomographic image.

3.3. MR images

MR images, after acquired, are usually stored and manipulated as a grid or matrix of points representing a slice, 2D image. These are matrices of pixels with *M* rows and *N* columns, where every pixel corresponds to a voxel and their information is normally codified in a digital image format.

The most typical format used for this is the Digital Imaging and Communications in Medicine, also known as DICOM-files. This is a very useful format because in addition to the MR image itself, it stores also information about the position and the orientation of the image regarding the MR scan and the patient.

For a 3D volume image, the scan acquires several slices, as shown in Figure 3.19, creating a 3D matrix with size *M* x *N* x *K*, where *K* represents the number of slices [12].

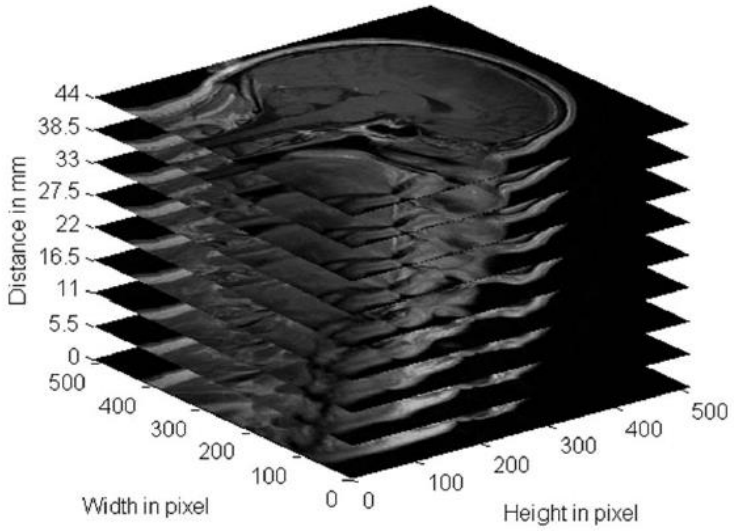

Figure 3.19 – MR image sequence with 5.5 mm spacing between slice **[12]**

But in real clinical practice, making images is an automatic process, with all gradients and timings pre-programmed in the MRI software. So this should create an ideal imaging technique with a rapid acquisition of data to provide good temporal resolution, high spatial resolution to resolve fine details of anatomy, and a high signal to noise ratio (SNR) to distinguish the tissues of interest by differences in the MR signal they generate.

Yet this does not happen. As spatial resolution is improved, the smaller image voxel generates a weaker signal relative to the noise. So high resolution images, with voxel volumes much less than 1 mm^3, could be acquired with standard equipment, what would lead to a Signal-to-Noise Ratio (SNR) so degraded that some anatomical information would be lost and as the voxel size decreases, the total number of voxels in the image increases, requiring a longer imaging time to collect the necessary information [22].

- Artefacts

Since it is almost impossible to ascertain the optimal conditions seen above, the images suffer some distortion, which are due to artefacts. Table 3 shows a list of some of these artefacts and these will be described next.

Table 3.3 – List of some artefacts that influence MRI **[23] [22] [12]**

Type	Artefact	Cause
Patient related	Motion	Voluntary or involuntary movements of the patient during the acquisition
Signal processing related	Chemical Shift	Mis-registration between the relative positions of two tissues with different resonance frequencies under an external magnetic field
	Partial Volume	Large voxel size
	Gibbs Phenomenon	Images with bright or dark lines adjacent to sharp boundaries duo to high spatial frequencies
Hardware related	Signal Noise	Bad RF shielding and operation of the RF coil and presence of metal in the patient
	B_0 Inhomogeneity	B_0 field distortion normally duo to metal objects in the patient

- **Motion**

During image acquisition, any movement performed by the patient, from the smallest movements of the head to the pulsing of blood vessels, will generate motion artefacts. These are responsible for a distorted analysis of the data series and not always their correction is possible through post-processing techniques. So, the application of realignment algorithms to the captured images to allow the obtainment of the geometric transformation function that is best suited to minimize differences between the images [22].

- **Chemical Shift**

It occurs at fat/water interface because of the frequency difference between the two components when under the influence of the external magnetic field. The protons of the fat tissue resonate at a slightly lower frequency then the water protons due to their different molecular structure.

The number of pixels affected by this artefact will depend of the frequency difference in Hz between the 2 components, the total receiver bandwidth and the number of readout data that cover the FOV. It can be determined and minimized shifting the phase-encoding and frequency-encoding gradients and examining the result or through the use of fat suppression techniques [23].

- **Partial Volume**

This artefact occurs when the size of the image voxel is larger than the size of the tissue of interest to be imaged, manly when multiple tissue types are comprised within a single voxel. That is, if a small structure is entirely contained within the slice thickness along with other tissue that has a different frequency, the resultant image will then have a signal correspondent to an average signal of the frequencies of both structures and this will cause a reduction of the contrast and loss of spatial resolution. So a solution for this problem could be a usage of a smaller pixel size or of a smaller slice thickness [23].

- **Gibbs Phenomenon**

This artefact is represented by the appearance of a series of lines parallel to a sharp intensity edge present in the image, normally borders of an abrupt intensity change which is caused by an incomplete digitization of the echo; in other words, where the signal has not decayed to zero by the of the acquisition window.

The Gibbs artefact can also be known as the truncation artefact because it results from the truncation of sampling in k-space, meaning an under-sampling of high spatial frequencies.

The methods used to solve this can be using a larger image matrix or filtering the k-space data prior to the Fourier transform [22].

- **Signal Noise**

This is referred to artefacts generated from unwanted signals resulting from multiple sources, normally from nearby electronic equipment that emit RF radiation that is captured by the head coil, causing significant noise in the acquired image [24].

- **B_0 Inhomogeneity**

This type of interference leads to errors in the mapping of the tissue because it can cause spatial and intensity distortions. The spatial distortion results from a long-range field gradient in B_0 that causes the spins to resonate at Larmor frequency different from the required. The intensity distortion is caused due to greater or smaller field homogeneity in a certain region than the imaged object [12].

3.4. Other techniques and applications

Some of the existing applications of this technology are:

- Standard MRI;
- Echo-planar imaging;
- *Fast Imaging with Steady-state Precession* (FISP);
- *Half Fourier Acquisition Single-shot Turbo spin Echo* (HASTE);
- Magnetic Resonance Angiography;
- Magnetic Resonance Spectroscopy;
- Functional MRI.

3.5. Summary

Magnetic Resonance Imaging produces tomographic images of internal physical and chemical characteristics of a given body by obtaining images and data sets representative of the multidimensional spatial distribution of a given physical quantity measure and these can be 2-dimensional (2D) sectional

images with any orientation, volumetric 3D images and even 4D images of the spatio-spectral or spatio-temporal distributions. These are captured with a scanner that has a static magnetic fields, uniform and strong and a computer used to control it and to process and present the results. This scanner analysis the Hydrogen composition of the body because it enables a stronger MRI signal.

The signal also depends on the Repetition Time and the Echo Time which can define the type of the image that is obtained and of a large variety of pulse sequences depending on the goals of imaging for the different applications, such as the identification of pathological body.

Another important concept that was acknowledged was the k-space selection responsible for some basic parameters of the image, such as the FOV, spatial resolution, etc., and the artefacts that affect the images that can cause some distortion.

4. Functional MRI

4.1. Introduction

The brain, like any other organ in the body requires a steady supply of oxygen in order to metabolise glucose to provide energy. This oxygen is supplied by the component of blood called haemoglobin that has magnetic properties which can be measured in a certain volume of oxygen present in the brain [17]. This volumetric dependency gave rise to a method for measuring the brain activation using MRI, commonly known as Functional Magnetic Resonance Imaging (fMRI) which will be approached in this next chapter.

4.2. Principles

The functional Magnetic Resonance Imaging is an application of the Magnetic Resonance Imaging referred to the use of this technology to detect localized changes in blood flow and blood oxygenation in the brain that occur in response to neural activity.

The concept that the cerebral blood flow could reflect neuronal activity began in 1890 with experiments carried out by Roy and Sherrington and this became the basis of all brain imaging techniques based on hemodynamic. In the last decades this technique has been greatly developed with the goal of mapping the human brain and has been extensively used to investigate the brain functions such as vision, language, motor and cognitive [22].

In 1990 Ogawa reported, based on their study in rat brains, that the mapping of functional brain was possible due to the BOLD effect (Blood Oxygenation Level Dependent) based on changes of deoxy-hemoglobin (dHb), where this acts as an contrasting parametric agent and whose local concentration changes in the brain leads to an increase in the intensity of the MRI signal [25].

Although the mechanisms which connect neuronal activation and brain physiology are still the subject of many studies, it is known that neuronal activation leads to an increased consumption of ATP (adenosine triphosphate), which implies an increase in oxygen demand and to fill this necessity an increase in local blood flow occurs and these physiological changes are

essential for fMRI. Thus, crossing the capillaries network, the oxy-hemoglobin (HbO_2) will release the oxygen it carries, becoming deoxy-hemoglobin (dHb), whose paramagnetic properties act to locally intensify the effects of external magnetic field. Therefore, to suppress this lack of O_2, there is an increase of local blood flow and volume, which leads to a further decrease in the concentration of dHb compared to basal level, and these changes in concentration of dHb act as contrast agent [24] [26].

Thus, according to Pauling & Coryell dHb is paramagnetic (attractive), that is, magnetizes in the same direction of the magnetic field to which it is exposed and HbO_2 is diamagnetic (repulsive) and these magnetic properties have a direct effect on the intensity of the detected signal in neural active regions. It can be verified that an increase in concentration of HbO_2 in blood flow will cause an increase in intensity of the captured signal and an opposite situation, namely in the presence of a higher concentration of dHb will lead to a decrease in local intensity due to the realignment of T2 and T2*. This occurs because the events that start with the increase of electrical activity and modulates the neurovascular response alter the MRI signal in time and produce the hemodynamic response function [27].

The fMRI techniques have evolved very rapidly over the past few years along with the development of analytical methods that can detect changes in neural activity. Therefore one of the main applications of fMRI is related to the field of neuroscience to allow a better study of the brain mechanisms as complex as perception, emotions, behaviour and pain, being of great interest to achieve quantitatively descriptions of these functions as well as qualitatively.

The fMRI fits well with these objectives because it involves a set of techniques that enables the exploration of the susceptibility of MRI signals to the physiological processes associated with brain activity [22].

4.3. Guidelines for fMRI experimental studies

For the analysis of fMRI a number of techniques derived from methods of processing and statistical analysis has been used. These can be classified as derived hypothesis and based on models or as derived data and exploratory.

The methods include model-based analysis of variance (ANOVA) and correlational methods and methods derived from data include principal component analysis (PCA) and Independent Components Analysis (ICA), all of which methods have as common factor the ability to identify the more meaningful areas of brain activation in a patient [28].

The fMRI studies are highly dependent on cerebral hemodynamic changes and for the organization of these are necessary to take into account the spatial and temporal characteristics of these hemodynamic effects. The spatial characteristics resulting from cerebral vasculature and the temporal characteristics relate to the inherent delay of signal changes in response to neural activity and the hemodynamic changes resulting dispersion over time.

Based on the temporal characteristics of the hemodynamic phenomena we can also classify the fMRI studies in [29]:

- **Delineation blocks**, where the experience is performed in continuous mode in blocks of time (typically lasting 20-60 sec) and whose purpose is to create a "steady state" of neuronal and hemodynamic changes. This is a good method for detecting small changes in brain activity. A schematic representation can be seen in Figure 4.1;
- **Delineation related with events** uses temporal response patterns and the hemodynamic response characteristics associated with the linear application of multiple stimuli. These last are applied individually and in random order and measure the hemodynamic response to each of them. This method may further divided into:
  - Design of spaced single study (with long intervals between stimuli and are used in order to allow that in the end of each stimulus the hemodynamic response returns to its resting state);
  - Design of fast single study (which takes advantage of the property of linearity and superposition of the hemodynamic response).

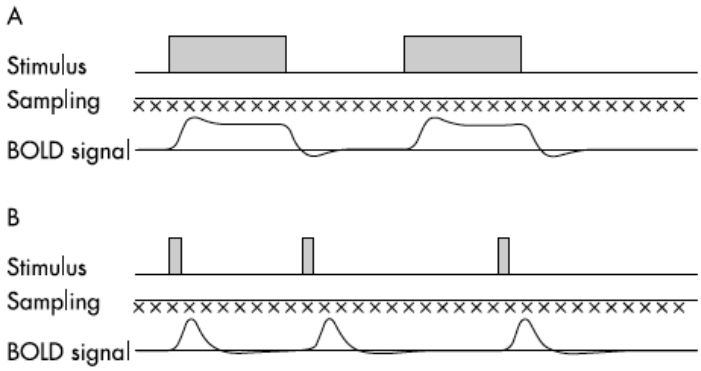

Figure 4.1 – Experimental designs for fMRI studies (A – block design, B – event-related design **[29]**

For these studies is also of extreme importance to know how to recognize the key variables to consider such as spatial resolution, temporal resolution, cerebral coverage and signal to noise ratio (SNR), so that they can be conveniently manipulated to obtain the desired results. Thus, to obtain a very high spatial resolution is necessary to reduce the temporal resolution, limit the coverage and reduce cerebral SNR.

However we must also consider other important aspects associated with these techniques, such as the extremely high financial costs and restrictions on patient safety [30].

For the BOLD fMRI studies, the most efficient design is the block design. According to Matthews and Jezzard “this design uses long alternating periods, during each of which a discrete cognitive state is maintained”. There has to be at least two different states alternating during the experiment in order to prevent that patient related artefacts or scanner sensitivity influence different impacts on the signal responses from both states [31].

4.4. Scanning methodologies

In an fMRI clinical study a large series of images is acquired while the patient is asked to do some tasks that make the brain activity shift between two or more well-defined states. The experimental procedure for the data acquisition can be described in a few general steps:

- the patient lies down, without moving, in a MRI scanner;

- next is the acquisition of the anatomical/structural scans of the brain (for about 6-15 minutes);
- then is a series of tests to collect the functional data between 3 to 10 minutes each (in these tests the patient will perform a few tasks that were pre-designed by the clinician. During the tests the scanner records the BOLD signal throughout the brain every each seconds.

This whole exam can take approximately 60 to 90 minutes and during it, several functional images are recorded each containing a large number of voxels, which constitute the time series of BOLD signals.

After this acquisition process the images are analysed with the goal to identify the brain areas that are significantly active during the experimental conditions compared to control conditions. This is made by correlating the signal time series in each voxel of a slice with the known time series of the test. [29].

4.5. Analysis of fMRI studies

The main goal in analysing functional imaging experiments is to identify the voxels that present signal changes that vary with the changing in brain states of interest on the acquired images.

The first step of this procedure is the pre-processing of the data consisting of:

- movement correction and realignment of the image series;
- spin history correction associated to head movements;
- spatial and temporal filtering;
- global intensity normalization;
- re-sampling of the data;
- re-ordering of the data [32].

Then, after the pre-processing step is complete comes the model fitting procedure where each voxel will be analysed in order to find voxel with time series correlated with the experimental conditions. The common process is to use mathematical functions to represent the BOLD response and estimate the data parameters [33].

The last step is the statistical inference in order to create a statistical parametric map, i.e. a brain image with voxels with their corresponding statistic values. This can be calculated through methods like:

- Gaussian random field theory;
- Permutation testing;
- Analysis at cluster level;
- Correction for multiple comparisons.

These steps are represented in Figure 29 [29].

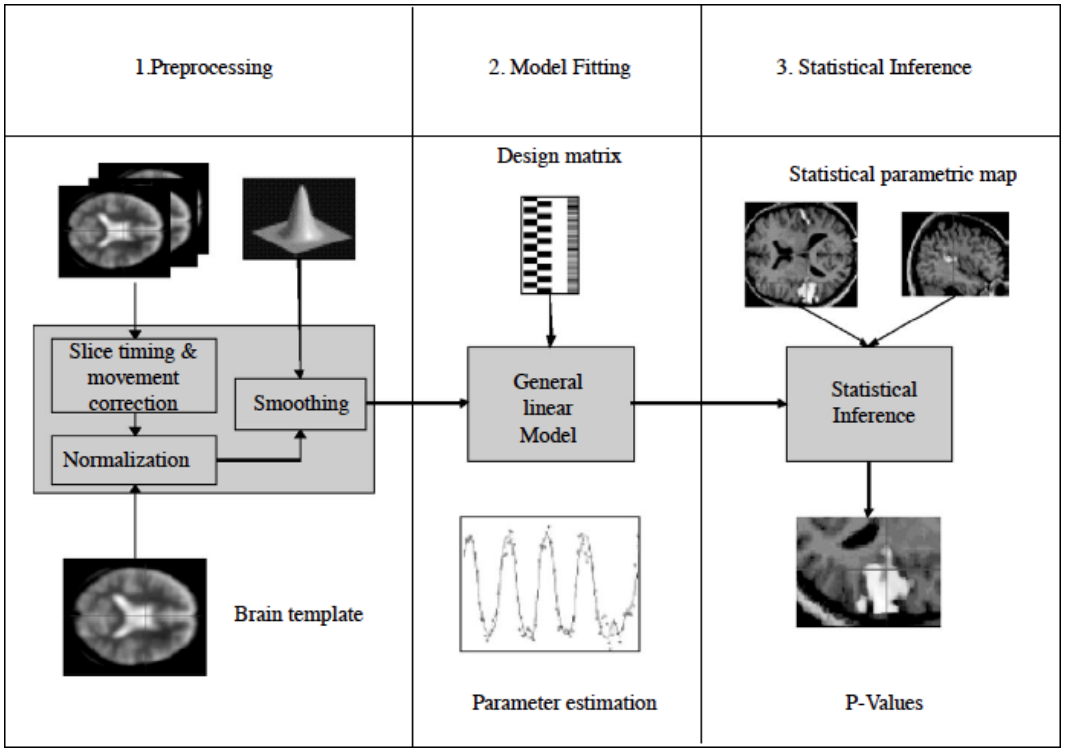

Figure 4.2 – Steps in fMRI data analysis **[29]**

For this purpose there are many different packages that already include a full set of tools for this analysis, like FSL (http://fsl.fmrib.ox.ac.uk/fsl), SPM (http://www.fil.ion.ucl.ac.uk/spm/) – that were used on this thesis – Analysis of Functional NeuroImages (AFNI) (http://afni.nimh.nih.gov/afni/), XBAM (http://www.brainmap.co.uk).

4.6. Limitations

Although fMRI is a very promising and useful technic it also presents a few limitations that need to be considered, not taking into account the artefacts referred in the previous chapter, inherent to this technic. These include:

- Large amount of images to evaluate;
- sensitivity to motion (patients head movements or brain microscopic movements);
- spatial and geometric uncertainty;
- poor temporal resolution;
- reduction of BOLD signal with proximity of brain lesions;
- large amount
- possible presence of false positives from the statistical analysis [34] [35].

4.7. Summary

The functional Magnetic Resonance Imaging is used to detect localized changes in blood flow and blood oxygenation in the brain that occur in response to neural activity and allows a better study of the brain mechanisms because it involves a set of techniques that enables the exploration physiological processes associated with brain activity. The studies developed to study this phenomenon can be delineation blocks or delineation related with events that take into account several key variables like spatial resolution, temporal resolution, cerebral coverage and signal to noise ratio (SNR), so that they can be conveniently manipulated to obtain the desired results. For a real fMRI clinical study a large series of images is acquired while the patient is asked to do some tasks that make the brain activity shift between two or more well-defined states and in these the main goal is to identify the voxels that present signal changes that vary with the changing in brain in order to obtain a statistical inference to create a statistical parametric map of the activity correspondent to the tasks preformed.

5. Image Processing and Analysis

5.1. Introduction

For a fMRI study is necessary to acquire one or more series of functional data (sequences of rapid MR), obtained during the performance of motor or sensory stimuli or during the performance of paradigms, which are sets of cognitive tasks, and acquisition of anatomical data (sequences of slow MR) covering areas of interest which serve as reference for the structural visualization of active functional areas. After this acquisition, the location and characterization of brain regions activated by stimuli is made. This requires several processing steps of the images since this process is subjected to the influence of several types of artefacts that can adulterate the acquired images [36].

According to Jenkinson & Smith [37] there is not only one protocol for the analysis of images of fMRI; however there is a base sequence of steps for processing images from fMRI:

1) Acquire and reconstruct the individual images;
2) Correct the time series phase for *timing* variations of the obtained cuts;
3) Apply a motion correction to correct head movements;
4) Spatial smoothing of data to increase SNR;
5) Filter each voxel's time series to remove temporal variations and high-frequency noise;
6) Perform the statistical analysis (through the generation of a statistical parametric map - a SPM)
7) Thresholding of SPM to find the significant active regions.

5.2. Image pre-processing – Artefacts removal

The contrast due to the BOLD effect combined with fast acquisition techniques, allows the visualization of certain brain processes. However, such contrast changes are not directly visible, which implicates the use of computational algorithms for the visualization of these same areas.

- **Motion correction:**

During image acquisition, any movement performed by the patient, from the smallest movements of the head to the pulsing of blood vessels, will generate motion artefacts. These are responsible for a distorted analysis of the data series and not always their correction is possible through post-processing techniques. So, the application of realignment algorithms to the captured images to allow the obtainment of the geometric transformation function that is best suited to minimize differences between the images [22].

One example of a possible approach is the use of Motion Correction FMRIB's Linear Image Registration Tool (MCFLIRT) algorithm used by the software package FMRI Brain's Software Library (FSL).

This algorithm is an image-similarity-based motion algorithm used on fMR time-series images. It is based on optimization and registration techniques from another fully automated tool for intra and inter-modal brain image registration, the FLIRT (FMRIB's Linear Image Registration Tool).

According to Jenkinson, M. et al, the algorithm, as in Figure 5.1, follows the next steps:

1) loads the entire time-series;

2) sets the middle image (V_n) as the initial image;

3) 8-mm optimization by identity transformation between V_n and the adjacent image (V_{n+1});

4) search for the optimal transformation (T_1) using the normalized correlation cost function;

5) consider the previous result as the starting point and follow the optimization for the next pair V_n, V_{n+2};

6) 4-mm optimization between V_n and the results from the previous optimization (as startup parameters);

7) 4-mm optimization with tighter tolerance between V_n and the results from the previous optimization;

8) apply the transformation parameters to uncorrected images.

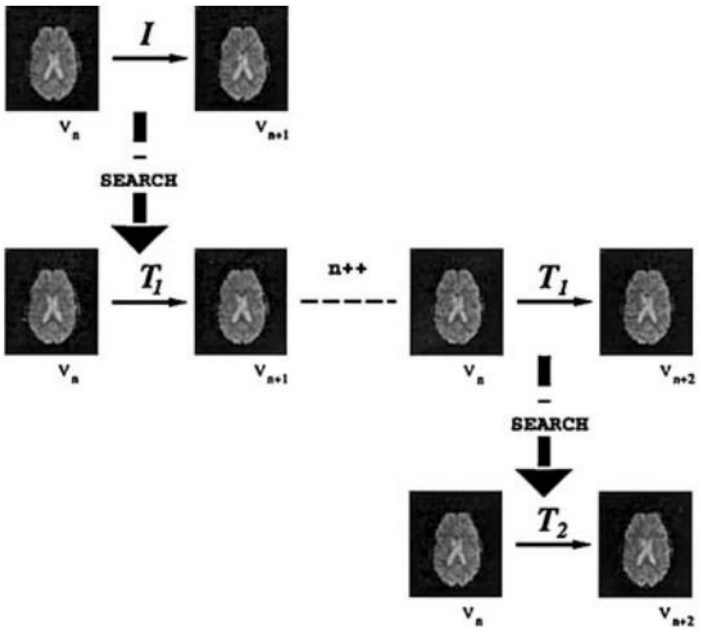

Figure 5.1 – Representation of the previous algorithm process **[37]**

- **Temporal correction**

The obtainment of temporal data series is performed by the acquisition of a cut at each time, which implies that different parts of the brain are not analysed simultaneously and that the data cannot be considered as an instant sample. Thus, for correcting this offset the data are adjusted through a displacement range of each temporal series of voxel's which can be done by applying an 1-D interpolation in the time domain or by applying a Fourier transform [36].

- **Spatial smoothing**

This step has as main goal the application of smoothing filters to reduce the distorting effects possibly caused by the instrumentation or even the physiological activity of the brain that can lead to the presence of noise. Thus for this purpose one resorts normally to low-pass filters, such as the 3D Gaussian filter, whose effects can be observed in Figure 5.2, to make a spatial smoothing of the temporal series of the fMRI data [36].

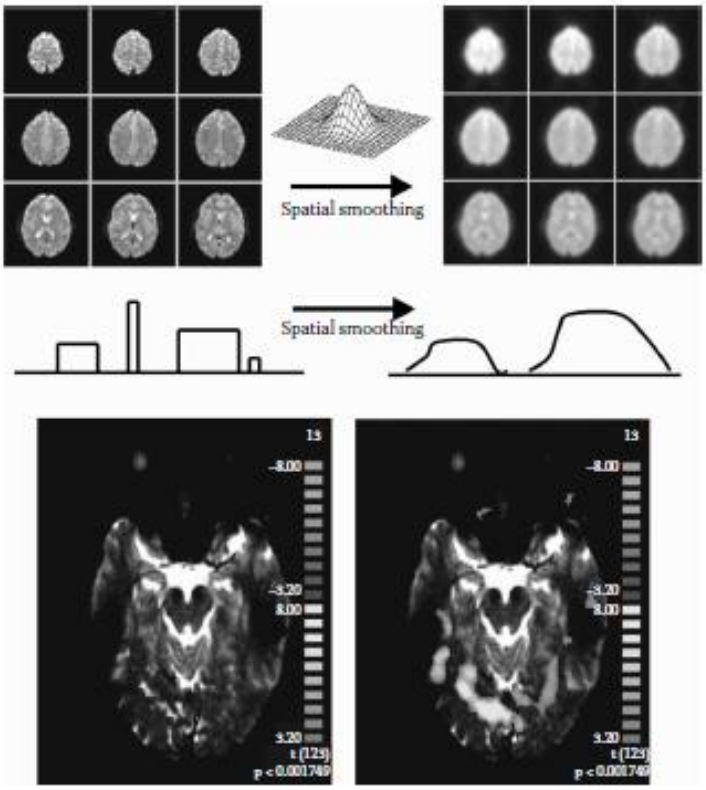

Figure 5.2 – Applying a 3D smoothing Gaussian kernel

This Gaussian filter has a normal distribution shape and once it is applied it spreads the intensity at each voxel in the image over nearby voxels. The voxels smoothed will depend on the size of the Gaussian kernel, i.e. the width of the curve; so if it is a narrow or a wide filter the response will be different, the wider the kernel the more voxels are affected by the data.

5.3. Image Enhancement

Image enhancement is a procedure used to bring out details that are blurred or to highlight features of interest in order to improve image contrast or their visualization allowing a better medical diagnosis.

There are two different domains of approaches possible for this procedure:

- Spatial domain methods;
- Frequency domain methods.

Nevertheless, this is a very subjective procedure as it is done for visual interpretation and this varies from operator to operator, as well as the concept of a quality image [38].

5.3.1. Spatial domain

Spatial domain approaches are directly based on the transformation of the image plane, that is the direct manipulation of the image pixels.

The general process of this method follows the mathematical expression:

$$\boldsymbol{g}(\boldsymbol{x},\boldsymbol{y}) = \boldsymbol{T}[\boldsymbol{f}(\boldsymbol{x},\boldsymbol{y})] \quad (5.1)$$

f(x,y) is the initial image, g(x,y) is the resultant image and T is the transformation operator that works over the (x,y) neighbourhood and this is the common base for many useful technics of this domain, like:

- Negative transformation images – these are the most basic operations in which the pixel values are inverted to generate de image negative;
- Thresholding transformations – where the image is converted to a binary image, with pixel values being 0 or 1 depending whether the initial values are higher or lower than an established threshold. This is a good approach to separate the objects of interest from the background.
- Histogram-based transformations – these are based on image histograms that are the graphical representation of the tone values of each pixel of an image and its adjustment or transformation allows the improvement of an image. This can be done by histogram equalization, histogram matching or the use of histogram to define a threshold [39].

5.3.2. Frequency domain

In the frequency domain case, the method applied is more straightforward regarding the noise reduction, because it can be easily identified in this domain.

This approach starts by computing the Fourier transform of the image in order to work in a frequency domain and the enhancement operations performed have the goal of improving image brightness, contrast or the distribution of grey levels. So the basic steps for these operations are illustrated in Figure 5.3 [38].

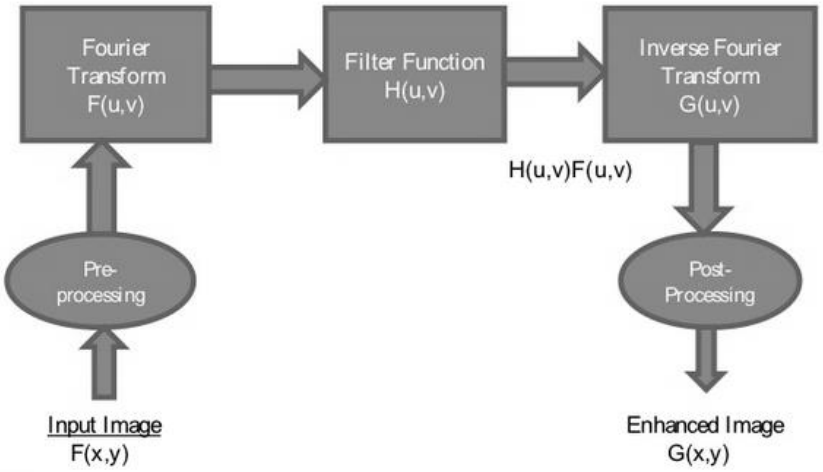

Figure 5.3 – Representation of the basic steps for frequency domain operations **[38]**

And from this we can establish that:

$$\boldsymbol{G(u,v) = H(u,v)F(u,v)} \tag{5.2}$$

Where G is the resultant image, F is the initial image and H is the transformation function.

So considering F(u,v) as the Fourier transformed image of F(x,y), this means that we have a set of different frequency values, where the low-frequencies normally correspond to smooth regions or blurred structures, and high-frequencies correspond to image details, edge or noise. So due to this defined difference it is possible to design specific filters according to the image frequency components:

- Low-pass filters – to smooth images through attenuation of high-frequency components;
- High-pass filters – to enhance image edges and sharp details through attenuation of low-frequency components [38].

5.4. Image Segmentation and Feature Extraction

The image segmentation process has a very important role in extracting useful information and attributes of images to analyse. This is one of the most important steps for the medical analysis, understanding and interpretation of images and its main aim is to divide them into homogeneous regions regarding certain criteria or characteristics. Each region can be processed separately to extract information. This process can be accomplished by identifying all the pixels or voxels falling within the same structure or region.

The segmentation of the images is not only important for the feature extraction and viewing but also for performing measurements and their comprehension.

The fMRI data segmentation is difficult to execute mainly due to the increased dimensionality of the data and the physical limitations imposed by this technique. The precise quantification of the regional physiology depends on the precise delineation (segmentation) of the structures or regions of interest (ROI) and the primary role of these are:

- Allow the quantification;
- Reduce the data set for analysis of the concentration of the extracted ROI;
- Establish a structural correspondence for physiological samples within regions.

A more direct approach to the segmentation is the manual delineation of ROI, but there are also semiautomatic methods that allow removing the subjectivity of this definition due to human operators.

5.4.1. Edge-based segmentation

This approach has two components for the determination of the borders and regions:

- Detection of the edges;
- Linking and monitoring of the edges.

These may be defined by the abrupt transitions in the intensity of pixels that can be given by the gradient information. The implementation of the detection of edges can be accompanied by the convolution of the original image with a mask (window or kernel) that will traverse the entire image. To resolve possible problems, duo to noise or artefacts failures of acquisition, the connection of the edges is then implemented to establish the connection between the pixels so the most significant edges are formed as well as closed regions.

5.4.2. Thresholding

It is one of the simplest technics to implement. In this, is selected a value (threshold) predefined and the image is divided into groups of pixels whose values are equal to or above the threshold and into groups with lower values. The most used approach is the Global Thresholding which is also simpler and computationally faster, but there are also other approaches such as the Local Thresholding and the Dynamic Thresholding. These last two are especially useful when the thresholding value cannot be determined from the histogram.

5.4.3. Region-based segmentation

This approach examines the pixels of the image and forms disjoint regions by union of neighbouring pixels with homogeneity property based on similarity criteria. The original image can be assembled by joining all regions without there being overlap between them. The simplest technique for this approach is the *Region Growing* which is used to extract the region of similar connected pixels in the image. This algorithm requires a similarity measure that determines the inclusion criteria of pixels and the stop criteria for stopping the growth of the region.

5.5. Summary

As has been discussed previously, fMRI studies need a certain amount of functional data such as sets of cognitive tasks and anatomical data of the active functional areas.

But before any data of interest can be extracted it is necessary to analyse this raw data that was acquired and for this there are predefined steps to be used: image pre-processing (motion correction, temporal correction, spatial smoothing), image enhancement (spatial domain and frequency domain), image segmentation.

In the case of images to aid the medical diagnosis the segmentation process has proven to be a very important step to extract information and attributes that can be useful like feature extraction and measurements. So regarding the detection of tumours the precise quantification of the regions of interest depends on its precise segmentation in order to obtain quantification and establish a structural correspondence for physiological samples within these regions.

Since there are various approaches to this process, it is important to study several different methods, the combination of different techniques and even different algorithms to test the extracted results of this analysis process are as accurate as possible and useful to aid in medical diagnosis.

6. Implementation, Results and Discussion

6.1. Introduction

6.2. Software and Data

6.3. Implementation and Results

6.4. Discussion

6.1. Introduction

This chapter starts with a brief introduction to the different software's that were used and the presentation of the data that was the object of study, followed by the presentation of the different methodologies implemented along the development of this thesis, their results and their respective evaluation and discussion.

6.2. Software and Data

For the development of this study, two different software's were used for the treatment of the same volume of data for later comparison of the results.

The programming was done in MATLAB Version 7.12.0.635 (R2011a) from Mathworks, Inc, with the Statistical Parametric Mapping (SPM), figure 6.1, version 8 from April 2009, developed by the Wellcome Trust Centre for Neuroimaging [40]. And the other software used was the FMRIB Software Library (FSL), figure 6.2, version 5.0 from September 2012, developed by the Analysis Group, University of Oxford, used through a virtual machine, the XQuartz 11, version 2.7.4, the X.org Foundation, Inc [41].

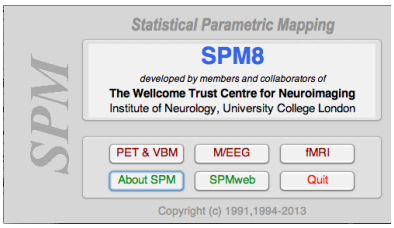

Figure 6.1 – SPM interface

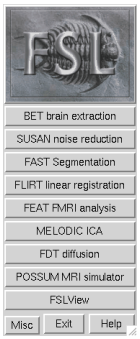

Figure 6.2 – FSL graphical interface

The data set corresponds to a functional magnetic resonance imaging study (fMRI) held at the clinical facilities of *Ressonância Magnética de Caselas*, acquired on a Sigma HDXT scanner from GE Medical Systems and whose characteristics are described in Table 6.1. This test was conducted to study the functional motor area, during which the patient was asked to open and close the hands for periods of 30 seconds interleaved with periods of muscle relaxation.

Table 6.1 – Main characteristics of the used Data Set

	Anatomical	**Functional**
Data set name	Axial FLAIR[1] T2	Hands
Size	256 x 256	64 x 64
Number of slices	32	3200
Slice thickness	4.0 mm	4.0 mm
Spacing between slices	1.5 mm	1.5 mm
Magnetic field strength	1.5 T	1.5 T
TE	122.8 s	24.5 s
TR	900.2 s	3000 s
Format	Dicom[2]	Dicom

A sample from the anatomical images series, in the axial plane, can be seen in figure 6.3.

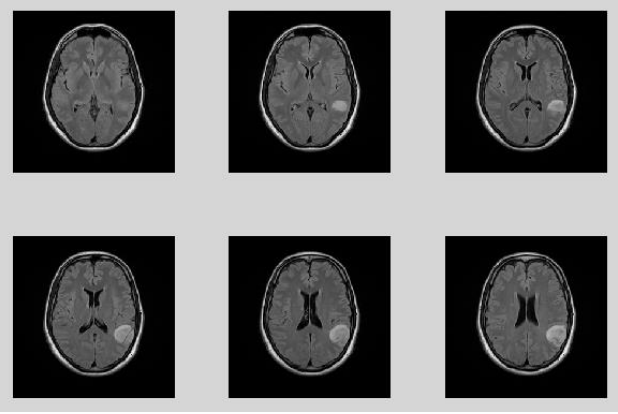

Figure 6.3 – Images from the T2 anatomical series in the axial plane (slices 15 to 20)

[1] FLAIR (Fluid attenuated inversion recovery) – T2-weighted images with cerebrospinal fluid suppressed.
[2] Dicom (Digital Imaging and Comunication in Medicine)

6.3. Implementation and Results

The processing of the images was quite different depending on the software used, but a common approach was kept for both and is represented in the diagram in figure 6.4.

Figure 6.4 – Representative approach for the common processing phases

The step of converting image formats is common to both software and was performed using software DCM2NII that allows the conversion of fMRI data in DICOM format to NIfTI format (Neuroinformatics Technology Initiative), a more compact and versatile format specific for the scientific analysis of brain imaging, which allows their use in the software's FSL and SPM.

Next will be explained the entire process of the practical stage and presented the results for each software.

6.3.1. FSL

As mentioned above, the FSL is a library of tools for fMRI, MRI and DTI data analysis with some specific functions already prepared for handling such data. Figures 6.5 and 6.6 show an example of anatomical and functional data, respectively, before the pre-processing phase.

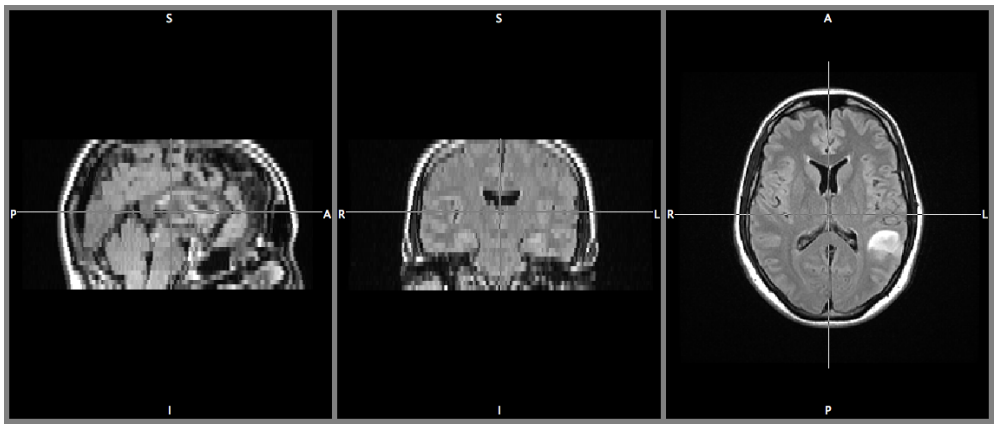

Figure 6.5 – Example of the anatomical images in the coronal, sagittal and axial planes

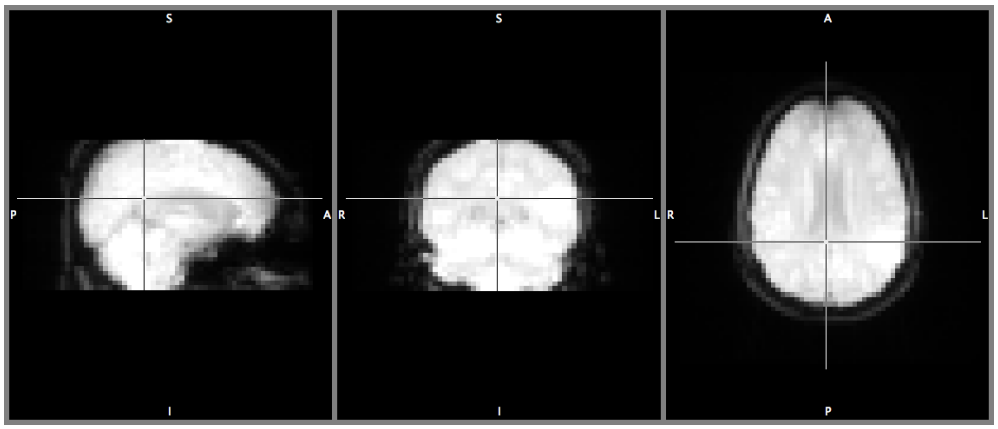

Figure 6.6 – Example of the functional images in the coronal, sagittal and axial planes

For this software, pre-processing, that is, the initial preparation of images for further processing more complex followed the following scheme (figure 6.7).

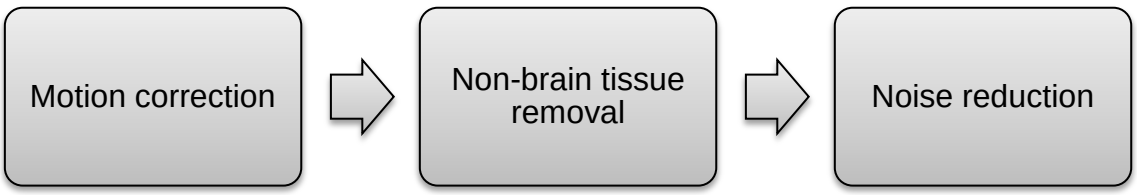

Figure 6.7 – Preprocessing procedure used in FSL

- Pre-processing stage
  - The motion correction was performed by intra-modal motion correction tool (MCFLIRT) of the FSL library, whose operation was explained in Chapter 5 [42].
  - Then there was the removal of non-brain tissue through Brain Extraction Tool (BET) that makes the automatic removal of the tissues corresponding to the outer surface of the skull and the scalp [43]. This tool has been tested for different values of fractional intensity threshold with the best result obtained for a value of 0.5 and it was also applied a gradient threshold of -0.1. The result of these two steps can be seen in Figures 6.8 (a and b).

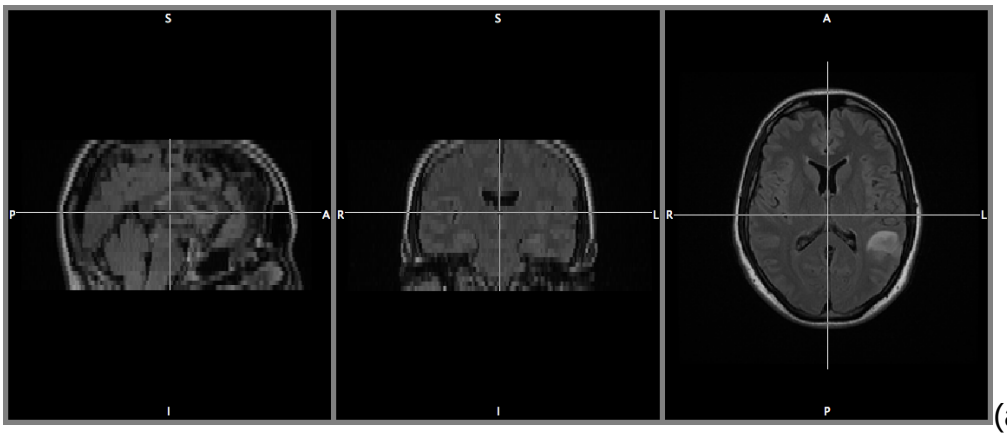

(a)

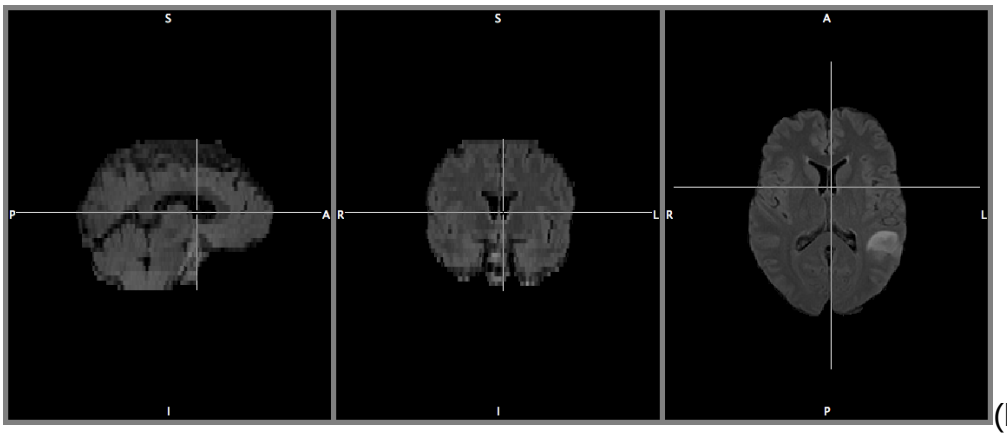

(b)

Figure 6.8 – (a) Motion correction result; (b) Non-brain tissue removal result

  - Finally, in this preprocessing stage a noise removal tool was applied, SUSAN (Smallest Univalue Segment assimilating Nuclues), a set of algorithms that allows the filtering of nonlinear

noise from series of images while preserving the structures through performing edge and corner detection, as it only averages a voxel that has local voxels with similar intensity. This was applied with a 3D dimensionality, brightness threshold of 207.18 and the use of a median filter when there is no neighbourhood [44]. The results of this filtering are more apparent in functional data represented in Figure 6.9 (a and b).

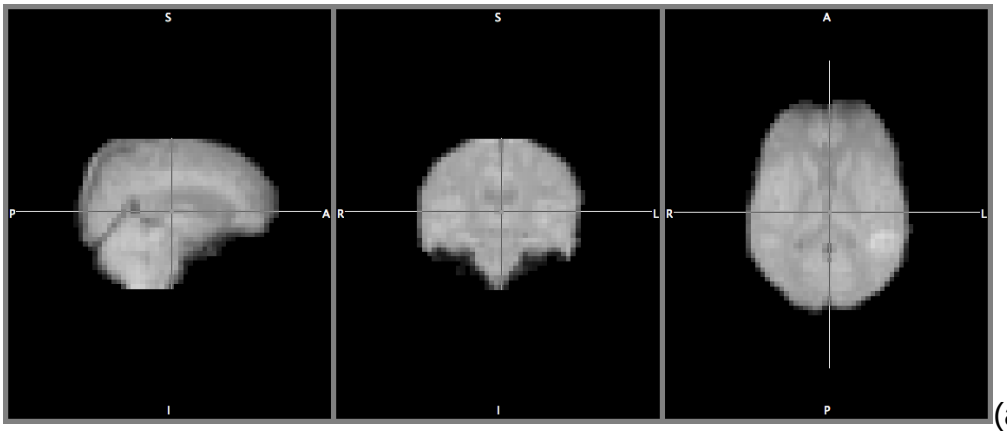

(a)

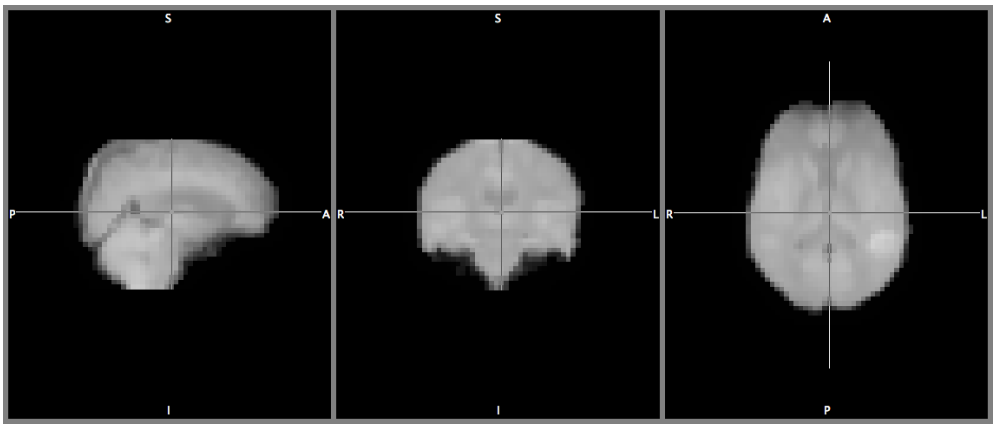

(b)

Figure 6.9 – Results from the noise removal stage (a – original, b – result)

- Segmentation stage

For this phase we used the FAST (FMRIB's Automated Segmentation Tool) tool, which based on a Markov random field model and an expectation-maximization algorithm allows to segment the brain images in different tissues present (grey matter, white matter, cerebrospinal fluid, etc.). In this case the anatomical images were segmented into four different classes, so that based on the intensity and contrast values was possible to segment the tissue

corresponding to the tumour, followed by the application of a gradient threshold values of intensity. The result of this phase can be seen in figure 6.10 [45].

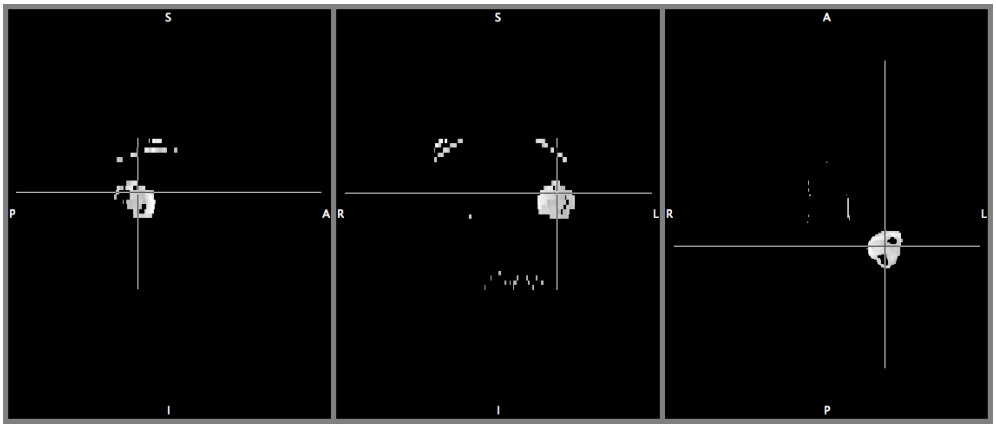

Figure 6.10 – Result of the FAST segmentation

Then a filter is applied to this space, based on the study of the coordinates of the tumour, which assigns zero to all voxels outside the region of interest, thereby defining the tumour (figure 6.11).

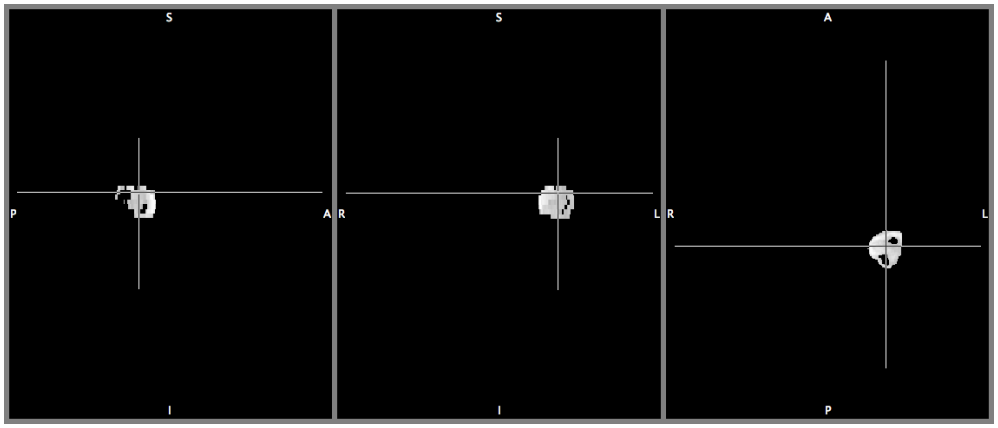

Figure 6.11 – Spatial filtering result

Finally we applied a dilation filter to fill the small holes within the region of interest, thus obtaining the final segmented tumor (Figure 6.12).

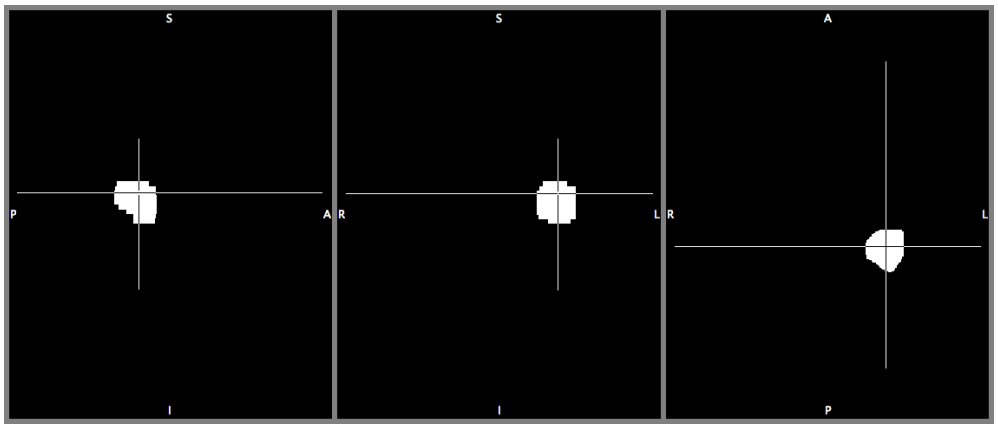

Figure 6.12 – Final result of the segmented tumour

- Functional Analysis

To analyze the functional data corresponding to the test performed to detect motor activation zone responsible for the action of the hand tool was used FEAT (FMRI Expert Analysis Tool) for the model-based fMRI data analysis. This tool is based on the general linear modeling (GLM) that enables manual description of the experimental design in this case a drawing represented in block diagram in figure 6.13 [46].

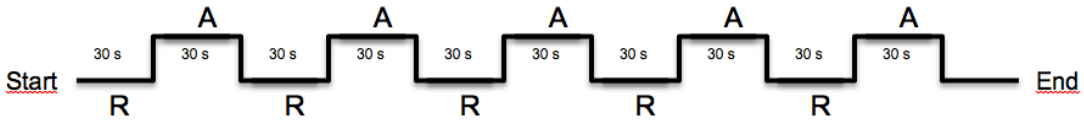

Figure 6.13 – Block diagram representative of the functional test (A – activation, R – rest)

This design, in which the activation period (A) corresponds to the action of opening and closing of the hands will then be compared with the data obtained so that it is possible to detect the brain regions that show activity in response to stimulus. For the data in question a first-level analysis was made, which is divided into 3 phases (Pre-statistical, Statistical and Post-statistical).

- Pre-statistical

In this phase was applied: MCFLIRT for motion correction; slice-timing correction using Fourier-space time-series phase-shifting; non-brain removal using BET, spatial smoothing using a Gaussian kernel with full width at half

maximum (FWHM) of 5 mm, grand-mean intensity normalization of the entire 4D dataset by a single multiplicative factor, the high pass temporal filtering with a Gaussian-weighted least-squares straight line fitting filter with a sigma of 30.0 s.

As a result of this first phase, we obtain the graphic of Figure 6.14 of the estimated average of the displacements of the patient during examination, and it was found the mean displacement (absolute of 0.19 mm and relative of 0.04 mm).

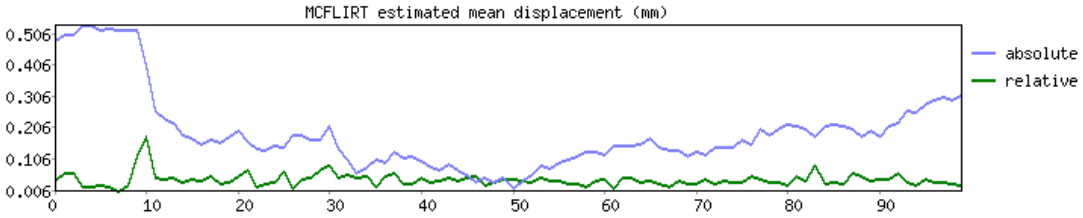

Figure 6.14 – Mean displacement estimation graphic

- Statistical

At this stage will be the time-series analysis based on the statistical block diagram used in this test so as to obtain the design matrix to be applied to data for the detection of activation. This result is shown in Figure 6.15.

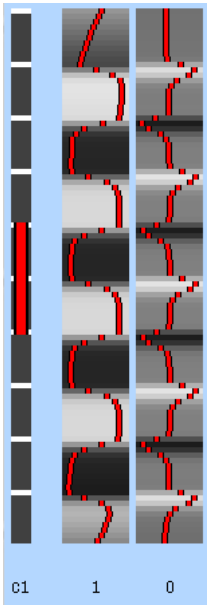

Figure 6.15 – Design matrix for the statistical analysis

- Post-statistical

Here the statistic images were thresholded using clusters determined by the condition Z> 3.0 and a cluster significance threshold of p = 0:05 to obtain the activation thresholded images of Figure 6.16 and the graphic of the time series of the Figure 6.17 which shows the correspondence between the model block applied and data collected activation.

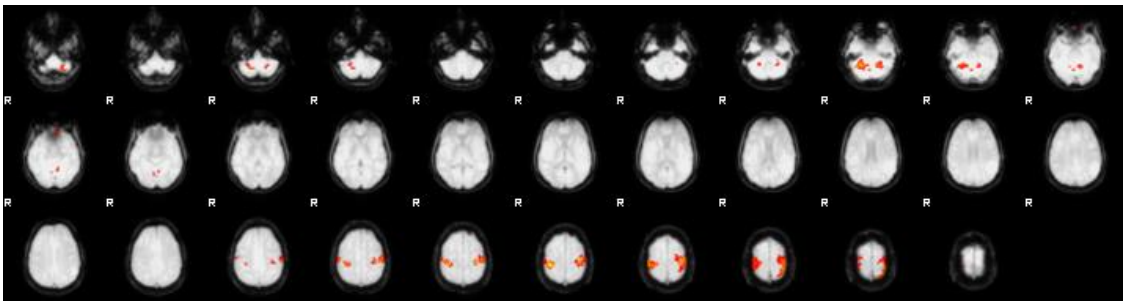

Figure 6.16 – Activation thresholded images

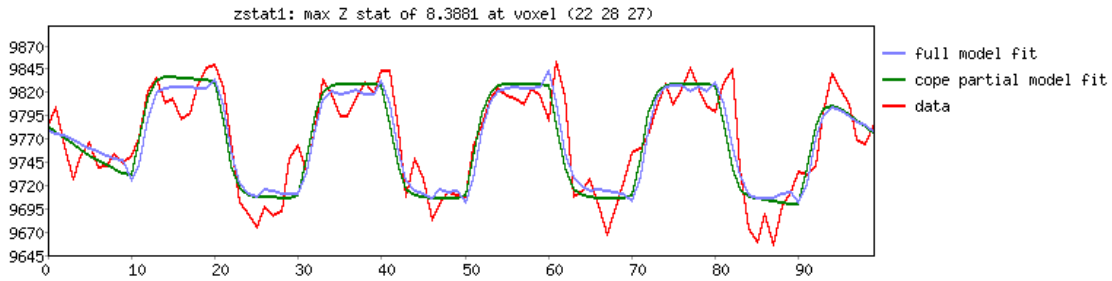

Figure 6.17 – Time series correspondence graphic

- Calculation of the distance between the edge of the tumor and the center of mass of the activation zone

To obtain the final aim was performed binarization of images of the zone of activation (Figure 6.18) to obtain the coordinates of the center of mass (x = 0.61, y = -13.29; z = 50.19 mm).

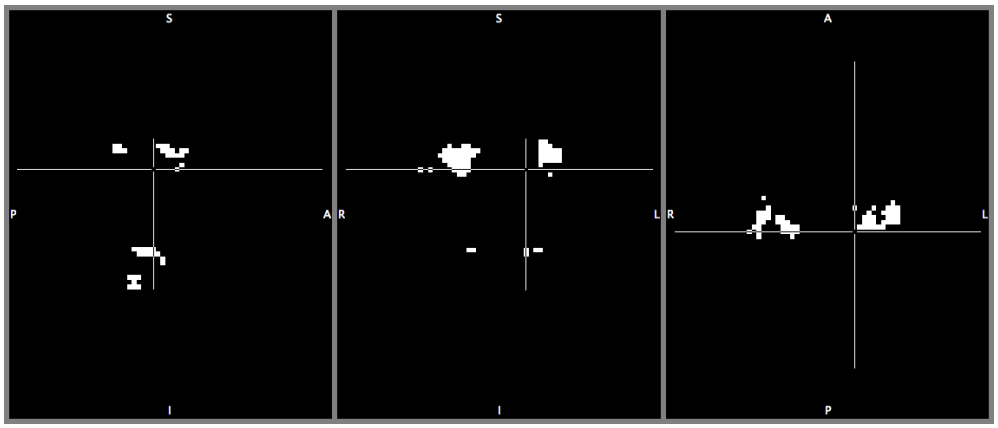

Figure 6.18 – Binarized activation area

Finally *distancemap* function was used to calculate all the distances between the point coordinates of the center of mass and the points on the periphery of the tumor, obtaining the minimum distance **d = 30.47 mm**.

6.3.2. MATLAB

The work developed in MATLAB was divided into three phases: a first phase where data were treated in their raw form, in DICOM format, for semi-automatic segmentation of the tumour; a second stage, using the SPM, for the treatment of the functional data, in NIfTI format, for obtaining the areas of activation and obtaining the coordinates of its centre of mass; and a third phase with the conjugation of the area corresponding to the tumour with the area of activation obtained, which allowed to obtain the coordinates of tumour closest point to the centre of mass for the final calculation of the distance between these two points.

- Phase 1

At this stage two algorithms have been developed for segmentation of tumour in anatomical images, both using the region growing method, one for the 2D segmentation and another 3D segmentation.

This method will group the pixels into regions according to the similarity between neighbour pixels. After defining the initial seed pixel, the algorithm will check which neighbour pixels satisfy the similarity criteria established (such as

intensity values) and will group them to create a region of interest. The process stops when the difference between the average values of the region and the new pixel exceeds a certain threshold set [38].

In figure 6.19 we can see the 2D segmentation result, initially developed for checking the correct selection of the region corresponding to the tumour.

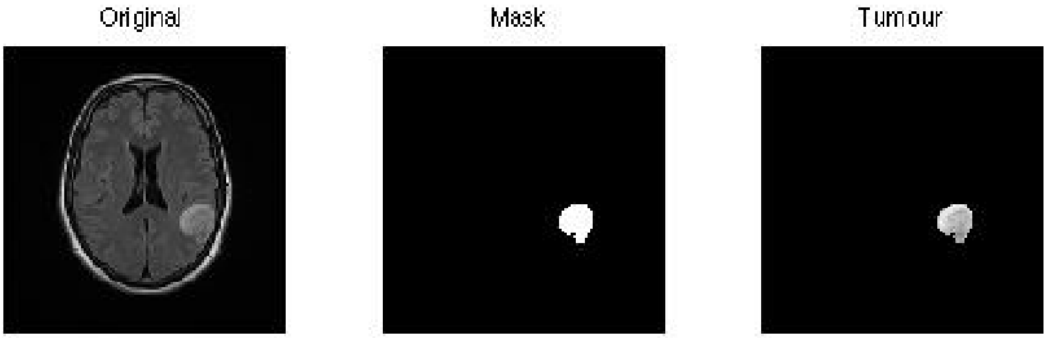

Figure 6.19 – 2D segmentation results

Then the algorithm was developed for the 3D segmentation of the tumour. This algorithm was also based on the Region Growing method. Here, the initial seed was selected on the preview data in 3D (Figure 6.20) to obtain the coordinates of a central pixel of the tumour and the result can be seen in Figure 6.21.

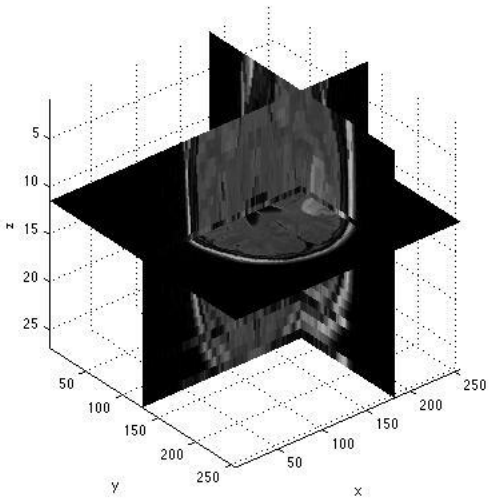

Figure 6.20 – 3D preview of the initial data

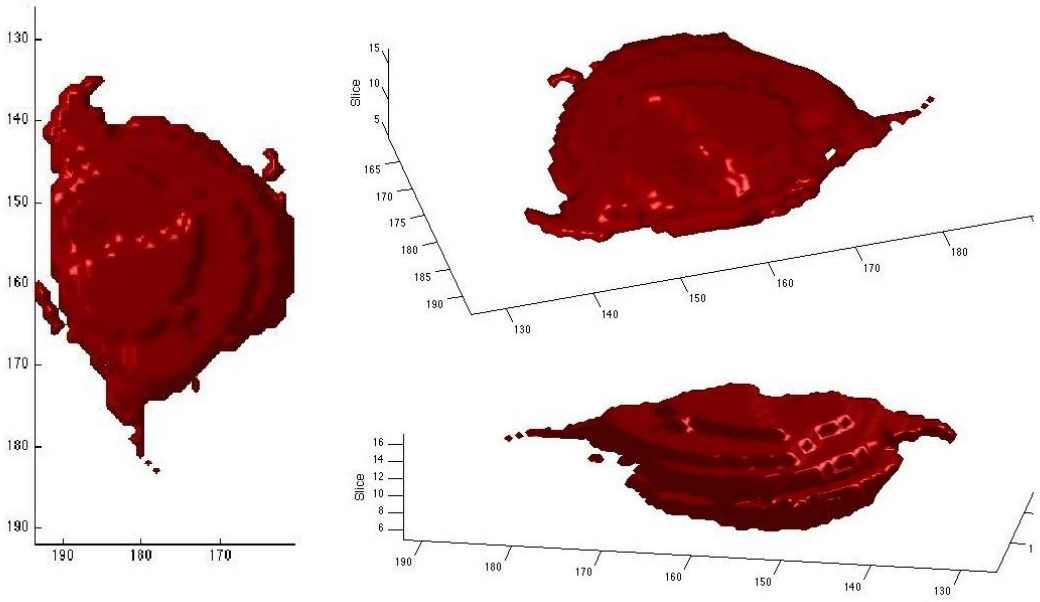

Figure 6.21 – 3D tumour segmentation result

- Phase 2

At this stage a first-level analysis to functional data was made. This analysis began with the pre-processing of functional data where they were subjected to the following steps: realign of the time-series images through a routine of SPM that uses a least squares approach and a 6 parameter spatial transformation. In this case, the first image of the series is the one that will be used as reference. Simultaneously, this routine will also remove motion artefacts inherent to this type of exams; smoothing of the data with a [8x8x8] Gaussian kernel in order to remove any noise present in the image volume [40].

After this pre-processing the first level functional analysis was done using a routine specific from SPM with the same experimental block design of Figure 6.13, and whose matrix applied this analysis is shown in Figure 6.22.

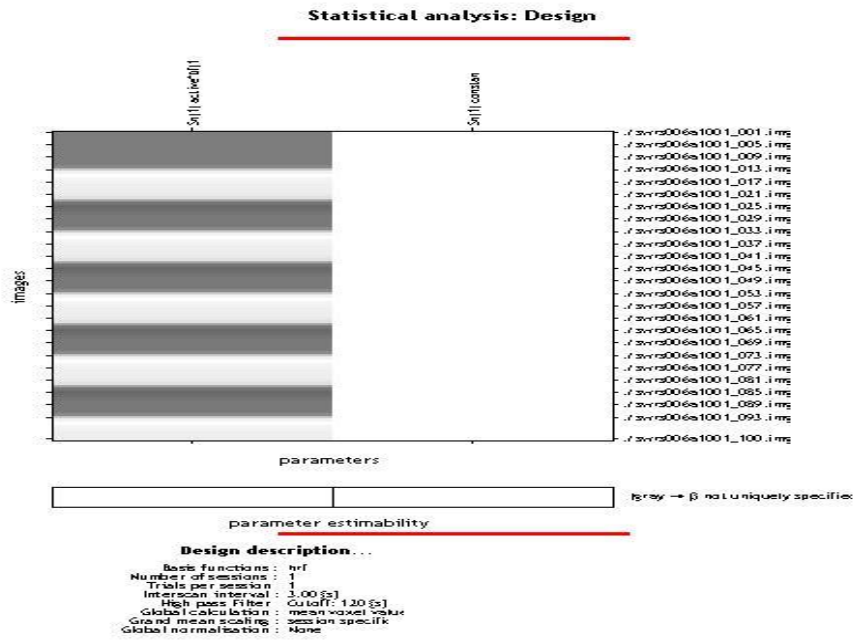

Figure 6.22 – Design matrix for the SPM statistical analysis

The final results of this analysis can be seen in Figure 6.23 where it is possible to see the table of estimated values for the formation of clusters and the location of areas of activation and Figures 6.24 and 6.25 is possible to see the difference in intensities in different areas of the brain.

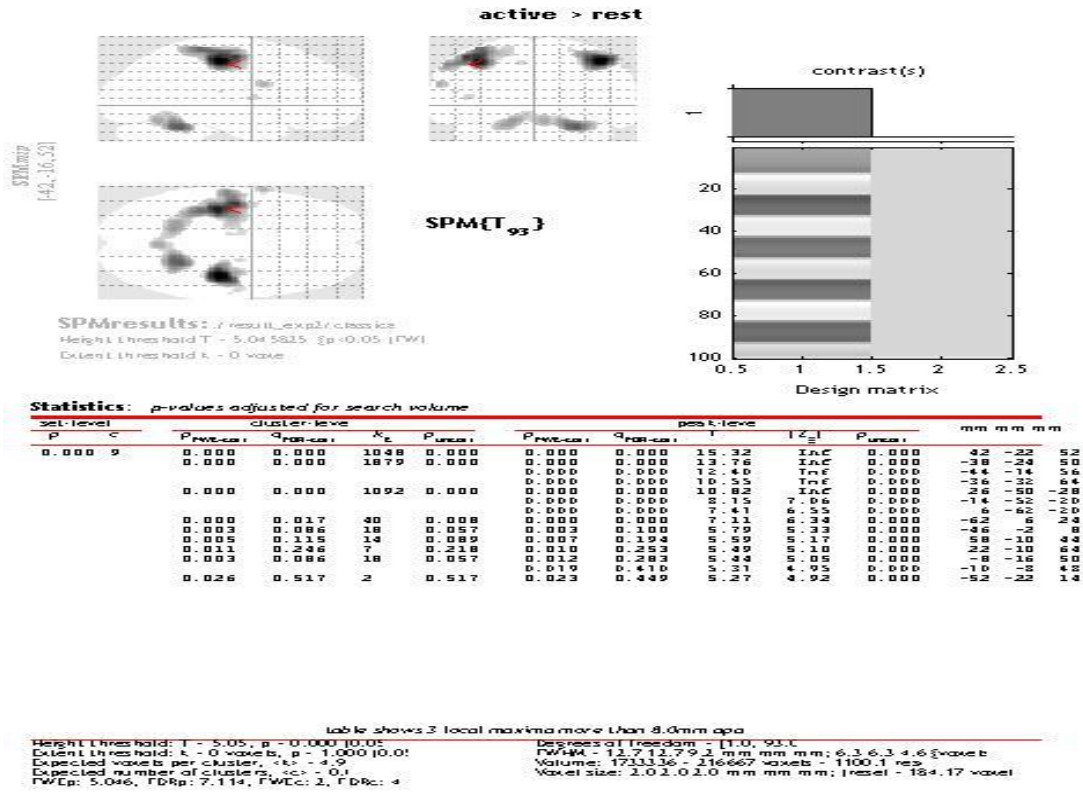

Figure 6.23 – Results with the clusters and activation zone locations estimated values

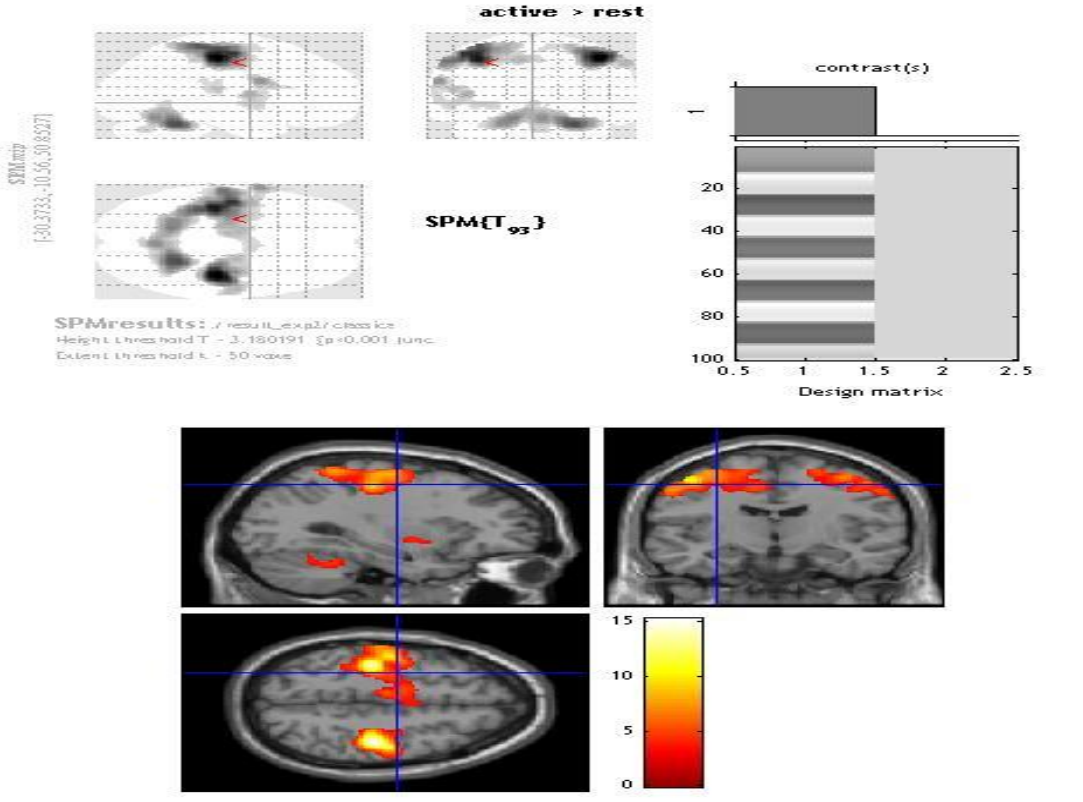

Figure 6.24 – Results with the diferente intensities of activation

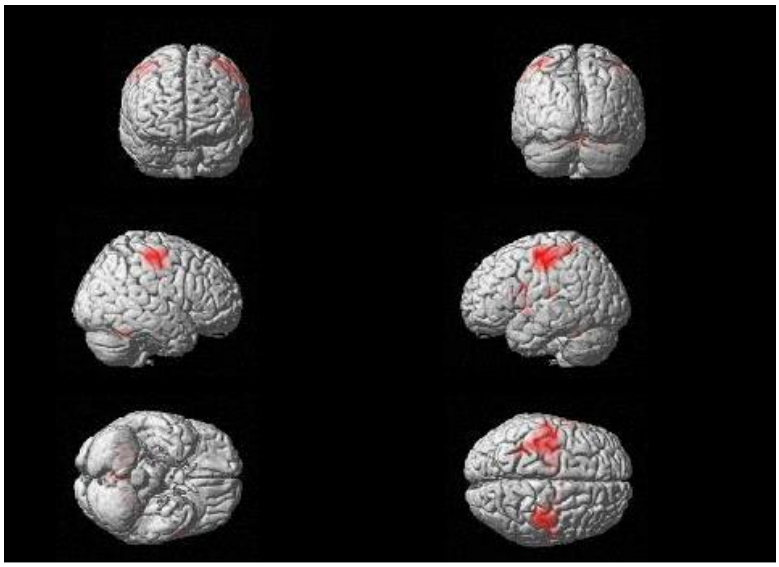

Figure 6.25 – 3D visualization of the location of the activation areas

After obtaining this statistical analysis, with the identification of the activation areas, region of interest was created corresponding to the location of these brain activations through the tool MarsBaR (Marseille Boite à Région d'Intéret) SPM, obtaining the results visible in Figures 6.26 and 6.27 in 3D [47].

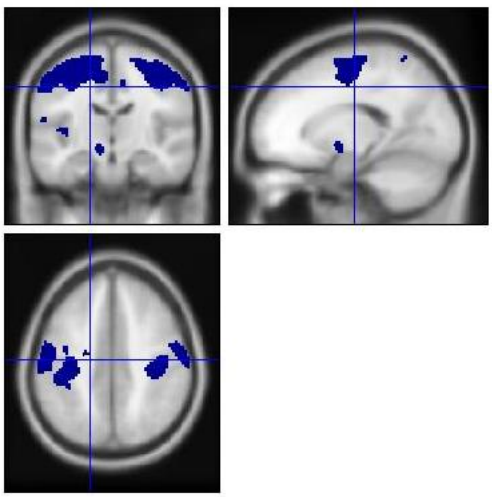

Figure 6.26 – Region of interest of the activation areas

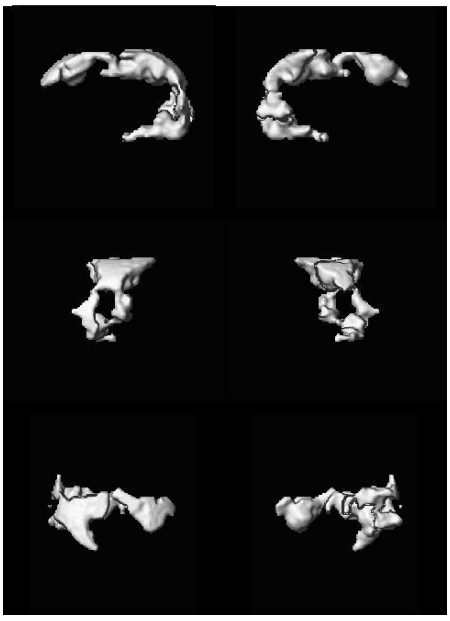

Figure 6.27 – 3D representation of the regions of interest

From Figure 6.26 it was possible to obtain information relating to the area of activation as the location of its centre of mass with the coordinates x = -17.5, y = -15.5, z = 42.1 mm.

Then using the same tool and the segmented tumour on the first stage was also obtained the region of interest corresponding to the tumour seen in Figure 6.28.

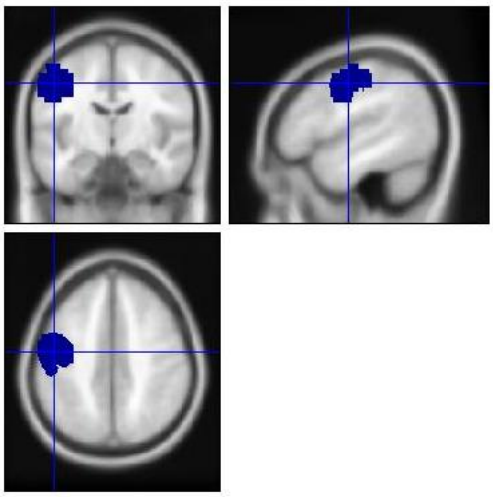

Figure 6.28 – Region of interest of the tumour area

- Phase 3

In this last phase, after combining the tumour region of interest with the coordinates of the centre of mass been we obtained ,with the same tool, the closest point between the tumour and centre of mass point, with the coordinates x = -31.8; y = -15.2, z = 35.3.

With these two sets of coordinates is possible to obtain the distance between them by use of the equation 6.1 to calculate the Euclidean distance:

$$d = \sqrt{(x_1 - x_2)^2 + (y_1 - y_2)^2 + (z_1 - z_2)^2}$$

Equation 6.1 – Euclidean distance

Thus was obtained a distance **d = 15.83 mm**.

6.4. Discussion

As can be seen there is a large discrepancy between the values obtained with the two different software's.

This may be due mainly to computation differences between the two software's and the different approaches made, considering the limitations of each.

In the case of FSL, as it is a specific software for statistical analysis of fMRI tests, it presents more limitations in the handling of anatomical images, that is, as the segmentation of the tumour process was based on a manual study of the tumour coordinates, it is possible that this has led to an imprecise segmentation, which in turn may partly explain this large difference in the distance values.

In the case of MATLAB, as this is a more powerful calculation tool it enabled the semi-automatic segmentation of the tumour, that is, less subject to errors of a user and as the SPM could use the results of this segmentation and conjugated them with statistical analysis of the data, is likely to have obtained a value for the distance more precise, despite the manual character of the final calculation.

Yet it is not possible to determine with certainty which value is more accurate, it would be necessary to obtain the opinion of a medical expert and analyse the results in every step of the process based on his professional experience.

It would also be useful to test these approaches in other data sets and observe the possible outcomes.

7. Conclusions and Future perspectives

For the study made for the measuring the distance between the edge of a tumour and the centre of mass of an activation area several reviews were carried out, from the brain anatomy and its pathologies, to the physics inherent in acquisition techniques of MR and fMR images, to the processing techniques of this kind of images that were the basis for the practical implementation of this work.

This study used two software's: FSL and MATLAB, with the testing of two different implementation approaches, to obtain the results.

The final results showed first that the two software's work very differently, and that the analysis of fMRI data, while being a statistical based study, requires a more complex analysis to better understand the discrepancy of values; and in second place that the segmentation techniques used require further refinement and validation of accuracy by a medical specialist. However, although this evaluation is not possible, one can say that the work is promising if continued its development, since the study of these distances can be used for the diagnosis and possible treatment of brain tumours without affecting the functional areas.

Two perspectives for future research would be the selection of one of the software's to work exclusively for testing more data volumes with medical validation and possible automation of the computational process.

References

[1] S. V. Madihally, Principles of Biomedical Engineering, Norwood: Artech House, 2010.

[2] J. L. Prince and J. Links, Medical Imaging Signals and Systems, Prentice Hall, 2005.

[3] J. T. Hansen, Netter's Clinical Anatomy, Philadelphia: Saunders, Elsevier, 2010.

[4] V. S. Ramachandran, Encyclopedia of the Human Brain, Academic Press, 2002.

[5] B. Cummings, “Chapter 12: Functional Areas of the Cerebral Cortex,” Austin Peay State University, [Online]. Available: http://www.apsu.edu/. [Accessed 10 January 2013].

[6] R. Seeley, T. Stephens and P. Tate, Anatomia & Fisiologia, 6ª ed., McGraw-Hill Companies, 2003.

[7] B. Greenstein and A. Greenstein, Color Atlas of Neuroscience: Neuroanatomy and Neurophysiology, Thieme, 2000.

[8] A. C. Poinier, “WebMD,” Healthwise Staff, 09 November 2010. [Online]. Available: http://www.webmd.com.

[9] Cancer Research UK, “Brain, other CNS and intracranial tumours incidence statistics,” 28 March 2013. [Online]. Available: http://www.cancerresearchuk.org/cancer-info/cancerstats/types/brain/incidence/#Distribution. [Accessed 17 April 2013].

[10] L. Tonarelli, “Magnetic Resonance Imaging of Brain Tumor,” [Online]. Available: http://www.cewebsource.com/coursePDFs/MRIBrainTumor.pdf. [Accessed 12 September 2012].

[11] M. Bethesda, “Adult Brain Tumors Treatment,” 2013. [Online]. Available: http://cancer.gov/cancertopics/pdq/treatment/adultbrain/HealthProfessional. [Accessed 14 April 2013].

[12] L. Landini, V. Positano and M. Santarelli, Advanced Image Processing in Magnetic Resonance Imaging, Boca Raton: Taylor & Francis Group, LLC, 2005.

[13] R. Khandpur, Biomedical Instrumentation: Technology and Applications, McGraw-Hill Professional, 2004.

[14] M. Kutz, Biomedical Engineering and Desing Handbook Volume 2: Applications,

McGraw-Hill Companies, 2009.

[15] J. D. Bronzino, The Biomedical Engineering HandBook, 2º ed., CRC Press, LLC, 2002.

[16] M. C. F. N. S. Hage and M. Iwasaki, "Imagem por ressonância magnética: princípios básicos," *Ciência Rural,* vol. 39, no. 4, pp. 1287-1295, 2009.

[17] A. A. Mazzola, "Ressonância Magnética: princípios de formação da imagem e aplicações em imagem funcional," *Revista Brasileira de Física Médica,* vol. 3, no. 1, pp. 117-129, 2009.

[18] R. K. Hobbie and B. J. Roth, Intermediate Physics for Medicine and Biology, Springer, 2007.

[19] J. D. Enderle, S. M. Blanchard and J. D. Bronzino, Introduction to Biomedical Engineering, Elsevier Academic Press, 2005.

[20] M. T. Vlaardingerbroek and J. A. Boer, Magnetic Resonance Imaging – Theory and Practice, 3º ed., Berlin: Springer, 2003.

[21] R. A. Pooley, "AAPM/RSNA Physics Tutorial for Residents: Fundamental Physics of MR Imaging," *Radiographics,* vol. 25, no. 4, pp. 1087-1099, 2005.

[22] R. B. Buxton, Introduction to Functional Magnetic Resonance Imaging - Principles and Techniques, 2º ed., Cambridge University Press, 2009.

[23] M. A. Brown and R. C. Semelka, MRI : basic principles and applications, 3º ed., New Jersey: John Wiley and Sons, 2003.

[24] S. H. Faro and F. B. Mohamed, BOLD fMRI - A Guide to Functional Imaging for Neuroscientists, New York: Springer, 2010.

[25] S. Ogawa, T. M. Lee, A. R. Kay and D. W. Tank, "Brain magnetic resonance imaging with contrast dependent on blood oxygenation," *Proceedings of the National Academy of Sciences,* vol. 87, pp. 9868-9872, 1990.

[26] P. Figueiredo, "O cérebro humano em actividade: investigação imagiológica por ressonância magnética funcional," *Gazeta de Física,* vol. 31, no. 1/2, pp. 8-12, 2008.

[27] L. Pauling and C. D. Coryell, "The magnetic properties and structure of hemoglobine, oxyhemoglobine and carbonmonoxyhemoglobine," *Proceedings of the National Academy of Sciences,* vol. 22, no. 4, pp. 210-216, 1936.

[28] P. Bogorodzki and J. Rogowska, "Structural Group Classification Technique based on Regional fMRI BOLD Response," *IEEE Transactions on Medical Imaging,* vol. 24, no. 3, pp. 389-398, 2005.

[29] P. Kenning, H. Plassmann and D. Ahlert, “Applications of functional magnetic resonance imaging for market research,” *Qualitative Market Research: An International Journal,* vol. 10, no. 2, pp. 135-152, 2007.

[30] R. Savoy, “Functional Magnetic Resonance Imaging (fMRI),” in *Encyclopedia of the Human Brain Vol.2*, Elsevier Science, 2002, pp. 327-350.

[31] P. M. Matthews and P. Jezzard, “Functional magnetic resonance imaging,” *Journal of Neurology, Neurosurgery and Psychiatry,* vol. 75, no. 1, pp. 6-12, 2004.

[32] E. Amaro Jr. and G. J. Barker, Study design in fMRI: Basic principles, Brain and Cognition, Elsevier, 2006.

[33] J. Jorge, W. Zwaag and P. Figueiredo, “EEG-fMRI integration for the study of human brain,” *NeuroImage,* vol. accepted, 2013.

[34] M. Smith, “Functional Magnetic Resonance Imaging (fMRI) in Brain Tumour Patients,” *European Association of NeuroOncology Magazine,* vol. 12, no. 3, pp. 123-128, 2012.

[35] P. Brandão and A. M. Reis, “Erro médico em imagiologia,” *Acta Médica Portuguesa,* vol. 19, pp. 235-238, 2006.

[36] E. Formisano, F. Salle and R. Goebel, “Fundamentals of Data Analysis Methods in Functional MRI,” in *Advanced Image Processing in Magnetic Resonance Imaging*, Taylor & Francis Group, LLC, 2005, pp. 481-500.

[37] M. Jenkinson and S. Smith, “The Role of Registration in Functional Magnetic,” in *Medical Image Registration*, CRC Press LLC, 2001, pp. 183-198.

[38] R. Gonzales and R. Woods, Digital Image Processing, 2º ed., Prentice Hall, 2002.

[39] R. Maini and H. Aggarwal, “A comprehensive review of image enhancement techniques,” *Journal of Computing,* vol. 2, no. 3, pp. 8-13, 2010.

[40] Guillaume, “SPM - Statistical Parametric Mapping,” Wellcome Trust Centre for Neuroimaging, 24 Junho 2013. [Online]. Available: http://www.fil.ion.ucl.uk/spm.

[41] S. Smith, “FSL - FslWiki,” Analysis Group, 11 06 2013. [Online]. Available: http://fsl.fmrib.ox.ac.uk/fsl.

[42] M. Jenkinson, P. Bannister and J. M. a. S. S. M. Brady, “Improved Optimisation for the Robust and Accurate Linear Registration and Motion Correction of Brain Images,” *NeuroImage,* vol. 17, no. 2, pp. 825-841, 2002.

[43] S. M. Smith, “Fast robust automated brain extraction,” *Human Brain Mapping,* vol. 17, no. 3, pp. 143-155, 2002.

[44] S. Smith and J. Brady, “SUSAN - a new approach to low level image processing,”

International Journal of Computer Vision, vol. 23, no. 1, pp. 45-78, 1997.

[45] Y. Zhang, M. Brady and S. Smith, “Segmentation of brain MR images through a hidden Markov random field model and the expectation-maximization algorithm,” *IEEE Trans Med Imag,* vol. 20, no. 1, pp. 45-57, 2001.

[46] M. Woolrich, B. Ripley and J. a. S. S. Brady, “Temporal Autocorrelation in Univariate Linear Modelling of FMRI Data,” *NeuroImage,* vol. 14, no. 6, pp. 1370-1386, 2001.

[47] M. Brett, J. L. Anton, R. Valabregue and J. B. Poline, “Region of interest analysis using an SPM toolbox,” *NeuroImage,* vol. 16, no. 2, 2002.